GEOFLUIDS
Geofluids (2015) doi: 10.1111/gfl.12133

Constraining groundwater flow in the glacial drift and saginaw aquifers in the Michigan Basin through helium concentrations and isotopic ratios

T. WEN[1], M. C. CASTRO[1], C. M. HALL[1], D. L. PINTI[2] AND K. C. LOHMANN[1]

[1]*Department of Earth and Environmental Sciences, University of Michigan, Ann Arbor, MI, USA;* [2]*GEOTOP and Département des Sciences de la Terre et de l'Atmosphère, Université du Québec à Montréal, Montréal, QC, Canada*

ABSTRACT

^{3}He and ^{4}He concentrations in excess of those in water in solubility equilibrium with the atmosphere by up to two and three orders of magnitude are observed in the shallow Glacial Drift and Saginaw aquifers in the Michigan Basin. A simplified He transport model shows that *in situ* production is negligible and that most He excesses have a source external to the aquifer. Simulated results show that ^{3}He and ^{4}He fluxes entering the bottom of the Saginaw aquifer are 7.5×10^{-14} and 6.1×10^{-7} cm^{3}STPcm^{-2} yr^{-1}, both of which are lower than fluxes entering the underlying Marshall aquifer, 1.0×10^{-13} and 1.6×10^{-6} cm^{3}STPcm^{-2} yr^{-1} for ^{3}He and ^{4}He, respectively. In contrast, He fluxes entering the Saginaw aquifer are higher than fluxes entering the overlying Glacial Drift aquifer of 5.2×10^{-14} and 1.5×10^{-7} cm^{3}STPcm^{-2} yr^{-1} for ^{3}He and ^{4}He, respectively. The unusually high He fluxes and their decreasing values from the lower Marshall to the upper Glacial Drift aquifer strongly suggest the presence of an upward cross-formational flow, with increasing He dilution toward the surface by recharge water. These fluxes are either comparable to or far greater than He fluxes in deeper aquifers around the world. Model simulations also suggest an exponential decrease in the horizontal groundwater velocity with recharge distance. Horizontal velocities vary from 13 to 2 myr^{-1} for the Saginaw aquifer and from 18 to 6 myr^{-1} for the Marshall aquifer. The highly permeable Glacial Drift aquifer displays a greater velocity range, from 250 to 5 myr^{-1}. While Saginaw ^{4}He ages estimated based on the simulated velocity field display an overall agreement with ^{14}C ages, ^{14}C and ^{4}He ages in the Glacial Drift and Marshall aquifers deviate significantly, possibly due to simplifications introduced in the He transport model leading to calculation of first-order approximation He ages and high uncertainties in Glacial Drift ^{14}C ages.

Key words: ^{14}C ages, Groundwater flow, helium ages, helium fluxes, sedimentary basin, tritium

Received 28 May 2014; accepted 19 February 2015

Corresponding author: Tao Wen, Department of Earth and Environmental Sciences, University of Michigan, 2534 C. C. Little Building, 1100 North University Ave., Ann Arbor, MI 48109-1005, USA
Email: jaywen@umich.edu. Tel: +1 734 730 8814. Fax: +1 734 763 4690.

Geofluids (2015)

INTRODUCTION

High salinity fluids are found at all depths in the Michigan Basin, from the deep Ordovician St. Peters Sandstone up to the shallowest subsurface levels (e.g., Glacial Drift, Long *et al.* 1988; Wilson 1989). The origin of such high salinities, however, remains uncertain and has been the focus of numerous studies (Long *et al.* 1988; Wilson 1989; Wilson & Long 1993a,b; Ging *et al.* 1996; Martini 1997; McIntosh *et al.* 2004, 2011, 2012; Ma *et al.* 2005). Upward transport of deep basinal brines and subsequent mixing with meteoric water has been previously proposed to account for the presence of high salinity groundwater in near-surface environments in the Michigan Basin (Long *et al.* 1988; Mandle & Westjohn 1989; Weaver *et al.* 1995; Kolak *et al.* 1999; McIntosh *et al.* 2004, 2011). Previous studies based on noble gases have confirmed the presence of upward cross-formational flow in the Saginaw and Marshall aquifers and deeper formations (Ma *et al.* 2005, 2009; Warrier *et al.* 2013). Helium, however, has not been previously used to investigate the presence of cross-formational upward transport in the shallowest formations of the Michigan Basin, that is, the Saginaw and Glacial Drift aquifers.

The study of noble gases in large-scale groundwater flow systems offers a powerful tool to investigate cross-formational flow within sedimentary basins as well as to track CO_2 leakage in natural CO_2-rich springs (Torgersen & Ivey 1985; Stute *et al.* 1992; Castro *et al.* 1998a,b; Pinti & Marty 1998; Castro & Goblet 2003; Patriarche *et al.* 2004; Holland & Gilfillan 2013; Warrier *et al.* 2013). Helium isotopes in particular can be used to ascertain whether or not cross-formational flow is occurring through the entire sedimentary sequence in the Michigan Basin and to better constrain the origin of the very high salinities present at all levels, and, more specifically, in shallow groundwater systems.

Because of its conservative nature, helium is transported by groundwater without reacting with the reservoir rocks. Typically, helium is present in the mantle, in the crust, and in the atmosphere (as a consequence of the degassing of the Earth). These components of different origin present specific characteristics, which allow identification of their sources and sinks (Stute *et al.* 1992; Hilton & Porcelli 2003; Castro 2004; Saar *et al.* 2005). Concentrations of He isotopes (^{3}He, ^{4}He) in groundwater frequently exceed those expected for water in solubility equilibrium with the atmosphere (air-saturated water: ASW). These excesses can result from different sources: (i) an excess air component resulting from dissolution of small air bubbles caused by fluctuations of the groundwater table (Heaton & Vogel 1981); (ii) the β-decay of natural background and bomb tritium (tritiogenic ^{3}He); (iii) the ^{6}Li(n, α)^{3}H (^{3}He) reaction (Morrison & Pine 1955) (i.e., nucleogenic ^{3}He); (iv) the α-decay of the natural U and Th decay series elements (i.e., radiogenic ^{4}He); and (v) mantle contributions to both ^{3}He and ^{4}He (e.g., Castro *et al.* 2009). A detailed analysis of both the helium concentrations and the ^{3}He/^{4}He (R) ratios measured in groundwater allows the separation of the different components. After separation of the individual He components, He isotopes can then be used to estimate mean water residence times.

Previous studies of the helium concentrations and isotopic ratios in the Marshall aquifer suggest the presence of tritiogenic ^{3}He in young groundwaters in this aquifer (Ma *et al.* 2005). High He excesses in old groundwater samples are mostly of crustal origin with the presence of a significant mantle He component in some samples. He excesses in the Marshall aquifer are unusually high for such a shallow depth and require a source external to the aquifer. Previous model simulations based on He data from the Marshall aquifer suggest the presence of high He fluxes at shallow depths within the Michigan Basin and point to the presence of a dominant vertical groundwater flow component, that is, upward leakage, and further suggest that the impact of the horizontal groundwater flow component (e.g., recharge water) at depth is minor (Ma *et al.* 2005).

Here, we present helium data and major ion chemistry from the two shallowest aquifers in the Michigan Basin, and the Glacial Drift and Saginaw aquifers, in addition to ^{14}C and tritium data for some samples in the Glacial Drift aquifer. These shallow groundwater data sets are subsequently analyzed in conjunction with helium data sets from the Marshall aquifer (Ma *et al.* 2005).

GEOLOGICAL AND HYDROGEOLOGIC BACKGROUND

Located in the northeastern United States, the Michigan Basin is a concentric intracratonic depression floored by crystalline Precambrian basement (Fig. 1A–C) and consists of a succession of sedimentary rocks from Precambrian to Jurassic that reaches depths of over 5 km (Dorr & Eschman 1970; Catacosinos & Daniels 1991). The entire sedimentary strata are covered by thick Pleistocene Glacial Drift sediments and are composed mainly of evaporites (e.g., Salina Group), carbonates (e.g., Traverse Formation), shales (e.g., Antrim and Coldwater Formations), and sandstones (e.g., Marshall Formation) (Fig. 1C). Depending on their nature, these sedimentary rocks constitute either aquitards (e.g., shale, evaporites) or aquifers (mostly sandstones and reefal and dolomitized limestones), giving origin to a multilayered aquifer system (Vugrinovich 1986; Westjohn & Weaver 1996a).

Major tectonic structures such as the Albion-Scipio Fault, the Lucas Fault, and the Howell Anticline (Fig. 1A) are present in southern Michigan and penetrate also the Precambrian crystalline basement (Fisher *et al.* 1988). The latter belongs to the Eastern Granite and Rhyolite Province (EGRP) and displays an age of ~1.5 Ga (William *et al.* 1975; Van Schmus 1992; Menuge *et al.* 2002).

The Marshall aquifer, a major groundwater flow system composed mostly of sandstones of Mississippian age, is located in the central portion of the Michigan Basin (Figs 1 and 2). The Bayport–Michigan confining units that are composed mostly of shale and limestone overlie the Marshall aquifer. The Marshall aquifer overlies the Coldwater and Antrim Shale confining units in turn (Fig. 1C). The Saginaw aquifer, a major groundwater flow system composed mostly of sandstones, is located in the central portion of the Michigan Basin (Fig. 1). It is underlain by the Bayport–Michigan confining units (Mandle & Westjohn 1989). These formations subcrop at an altitude of ~275–300 m and are overlain by the unconfined Glacial Drift aquifer that consists dominantly of thick sequences of glacial and/or fluvial sand and gravel that covers most of the Michigan Basin (Westjohn *et al.* 1994; Hoaglund *et al.* 2002).

In the Glacial Drift aquifer, groundwater in southern Michigan flows NW and NE into Lakes Michigan and

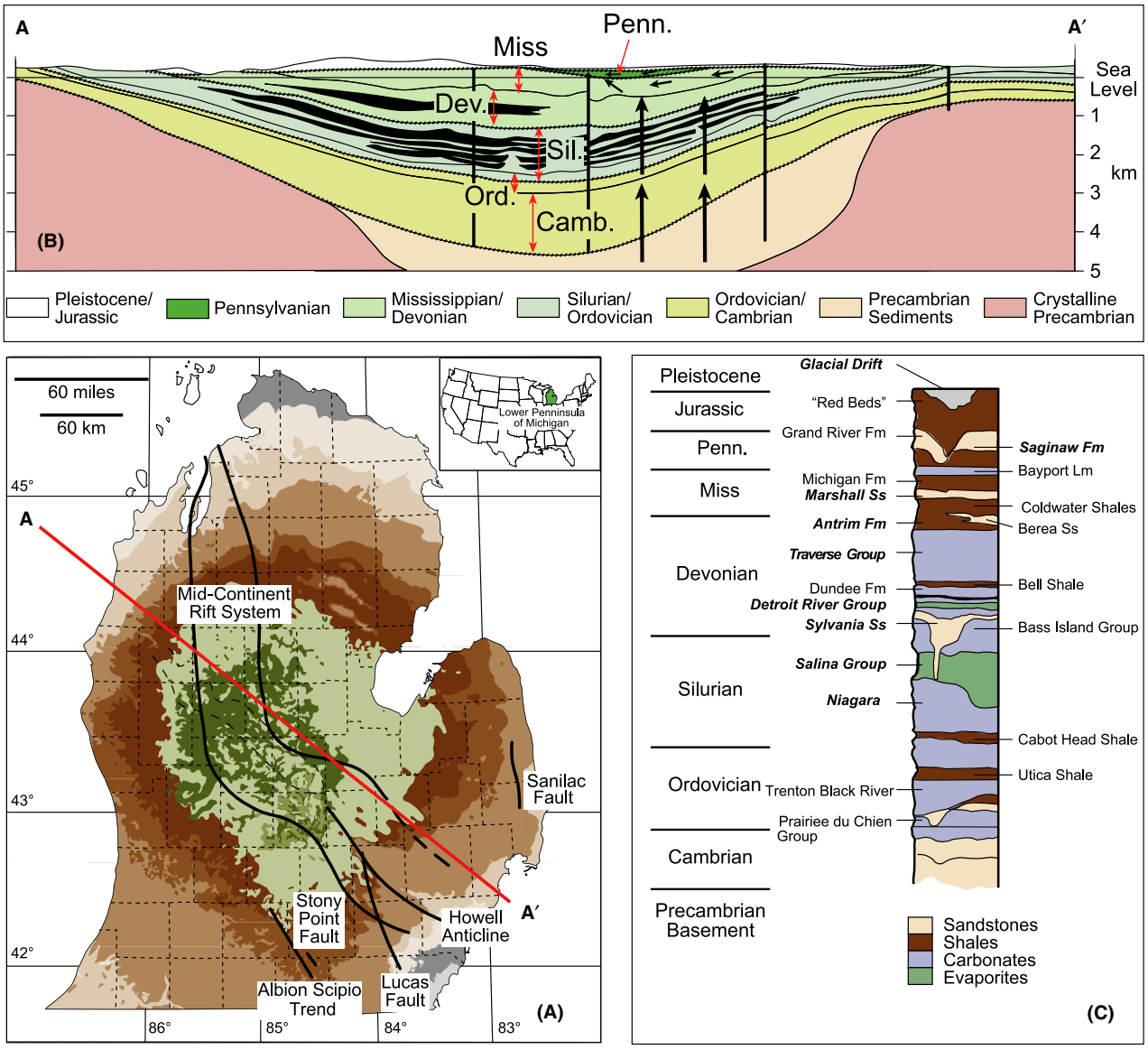

Fig. 1. Hydrogeologic framework of the study area. (A) Subcrop formations and major structures present in the Michigan Basin—Lower Peninsula of Michigan (after Dorr & Eschman 1970; Fisher *et al.* 1988); horizontal groundwater flow (small arrows) in the Marshall, Saginaw, and Glacial Drift aquifers and vertical upward fluxes entering these aquifers (long arrows) are also indicated; (B) General schematic geologic representation along cross section A–A′; (C) stratigraphic succession through the Michigan Basin in which major lithologies present in the basin are identified; units for which He data of formation groundwater are discussed in this study are indicated (bold italic).

Huron, respectively (Fig. 2). In northern Michigan, groundwater flows gravitationally toward the SW and SE into Lakes Michigan and Huron, respectively (Fig. 2). In the Saginaw aquifer, groundwater flows gravitationally mainly from the south to the NE and from the north to SE into the Saginaw Lowlands (SL) region and Lake Huron, where it discharges (Fig. 2). In the Marshall aquifer in southern Michigan, groundwater flows gravitationally to the NW and NE and discharges into Lakes Michigan and Huron (SL area), respectively (Vugrinovich 1986; Mandle & Westjohn 1989). A detailed description of the aquifer characteristics and regional geohydrology of the Michigan Basin aquifers is available elsewhere (Vugrinovich 1986; Mandle & Westjohn 1989).

During the Pleistocene glacial advances (e.g., Wisconsinan, Illinoian, Kansan), the Michigan basin was entirely covered by ice sheets (Dorr & Eschman 1970; McIntosh *et al.* 2011). In general, the ice sheet advanced from north to south across the Michigan Basin and retreated toward the north (McIntosh *et al.* 2011; Castro *et al.* 2012). Glacial loading of the Laurentide Ice Sheet (LIS) during the last glacial maximum (LGM, ~18 ka)

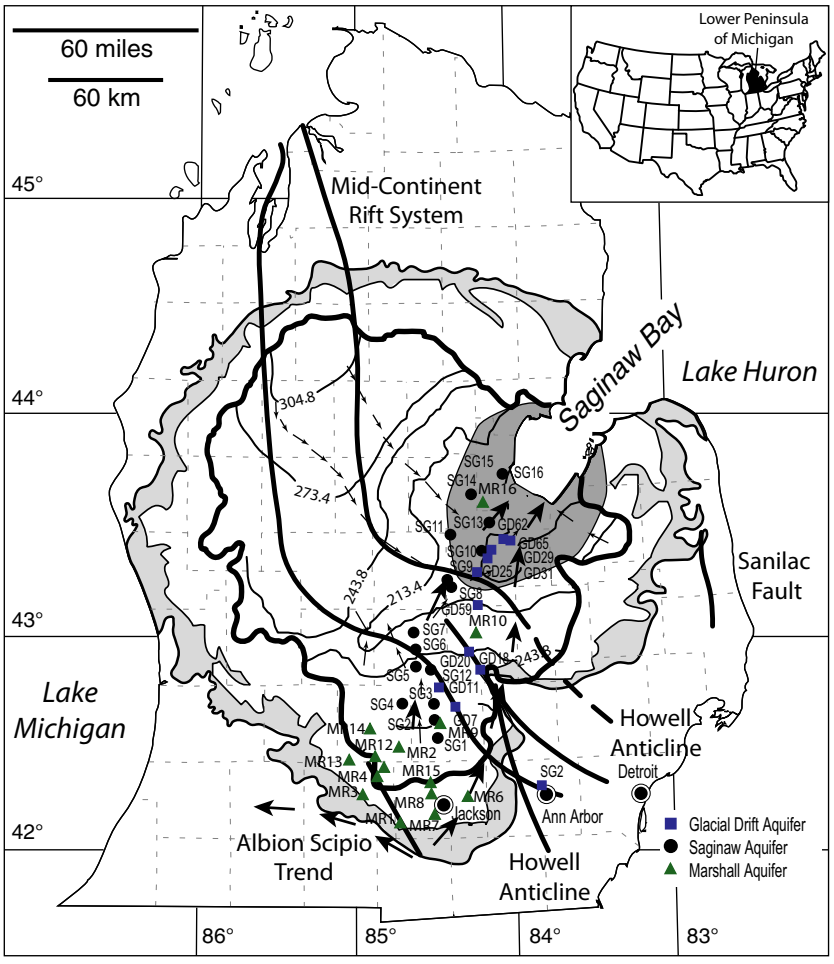

Fig. 2. Detailed study area and location of the Glacial Drift (dark blue squares), Saginaw (black circles), and Marshall (green triangles) aquifer samples in southern Michigan (adapted from Mandle & Westjohn 1989). Bold contour represents the Saginaw subcrop; gray contour represents the Marshall subcrop. Equipotential line (contour lines) values are shown in meters together with main groundwater flow directions (small arrows) for the Saginaw aquifer (Castro *et al.* 2012). Dark gray area corresponds to the Saginaw lowlands. Regional groundwater flow direction for the Glacial Drift aquifer (large arrows) is also shown.

dramatically increased the hydraulic heads in the Michigan Basin aquifers, thus reversing the regional groundwater flow pattern in northern Michigan and SL areas (Hoaglund *et al.* 2004; Person *et al.* 2007; McIntosh *et al.* 2011). Similar reversals were also identified east of the Michigan Basin and the nearby southeastern Wisconsin (Klump *et al.* 2008; Neuzil & Provost 2014). Following the retreat of LIS, groundwater flow rapidly resumed to observed modern patterns (Hoaglund *et al.* 2004; McIntosh *et al.* 2011).

Predevelopment freshwater heads (Barton *et al.* 1996), groundwater flow simulations (Hoaglund *et al.* 2004; McIntosh *et al.* 2011), and high helium fluxes in the Marshall aquifer, as well as dissolved major elements throughout the entire sedimentary aquifers (Ma *et al.* 2005), point to the presence of an upward cross-formational flow in the SL area. Cross-formational flow appears to be particularly significant in the lower formations and is likely responsible for the presence of extremely high salinity values (total dissolved solids—TDS ≥ 200 g l^{-1}) in the Marshall aquifer in this region (Ma *et al.* 2005).

SAMPLE COLLECTION AND MEASUREMENTS

A total of 22 groundwater samples were collected from 11 wells (2 duplicates at each well site) in the Glacial Drift aquifer for analysis of concentrations and isotopic ratios of all stable noble gases (He, Ne, Ar, Kr, Xe) after temperature and pH reached equilibrium. Samples were collected in copper tubes (i.e., standard refrigeration grade 3/8" Cu tubing) and water was allowed to flow through for ~10 min. While the water flushed through the system, the absence of gas bubbles that could potentially contaminate or phase fractionate the samples was checked through a transparent plastic tube mounted at the end of the Cu tube. The Cu tubes were then sealed by stainless steel pinch-off clamps (Weiss 1968). Noble gases were analyzed at the Noble Gas Laboratory at the University of Michigan as described briefly below and in detail by Warrier *et al.* (2012) and Hall *et al.* (2012). Water samples in Cu tubes were attached to a vacuum extraction system, and noble gases were quantitatively extracted for inletting into a MAP-215 mass spectrometer. Noble gases were transported using water vapor as a carrier gas through two

constrictions in the vacuum system, purified, and sequentially allowed to enter a MAP-215 mass spectrometer using a cryoseparator. The complete measurement procedure comprises estimation of He, Ne, Ar, Kr, and Xe concentrations, and their respective isotopic ratios, with standard errors for volume estimates of 1.5%, 1.3%, 1.3%, 1.5%, and 2.2%, respectively. When replicate analyses are available, an error-weighted average is reported. Excess air (EA) was calculated from measured noble gas concentrations using the unfractionated air (UA) model (Ballentine & Hall 1999; Kipfer *et al.* 2002).

Seven groundwater samples were also collected for analyses of major elements in the Glacial Drift aquifer. These were filtered with a 0.45-μm Gelman Laboratory AquaPrep filter and subsequently preserved in high-density polyethylene bottles with no headspace before analysis. Samples for cation analyses were acidified to pH <2 by using nitric acid. Major ion chemistry of these samples was determined in the Aqueous Geochemistry and Hydrogeology Laboratory at the University of Arizona. Alkalinity was measured by the Gran-Alkalinity titration method (Gieskes & Rogers 1973) with a precision of ±1%. Cation chemistry was determined by inductively coupled plasma-optical emission spectrometer (ICP-OES) with a PerkinElmer Optima 5100DV (precision, ±2%). Anions were analyzed by ion chromatography (IC) with a Dionex Model 3000 (precision, ±2%). Groundwater ages for 7 samples in the Glacial Drift aquifer were calculated from ^{14}C activities measured at the AMS facility at Woods Hole Oceanographic Institution. Corrected ^{14}C ages from the Mook model (Mook *et al.* 1974) for all Glacial Drift samples were subsequently converted into calibrated calendar ages using CALIB Rev6.1.0 program (Stuiver & Reimer 1993; Castro *et al.* 2012) and IntCal'09 calibration data set (Reimer *et al.* 2009). Calibrated calendar ages are referred to hereafter simply as ages.

3 Glacial Drift samples for tritium analyses were collected in copper tubes following the same collecting protocols for the noble gas samples and subsequently measured in the Noble Gas Laboratory of Lamont-Doherty Earth Observatory. Tritium concentrations were measured by ^3He ingrowth method with a precision of ±2% and a detection limit of 0.01 TU (Ludin *et al.* 1998).

Groundwater samples from 16 wells in the Saginaw aquifer were also previously collected and analyzed for noble gas concentrations (He, Ne, Ar, Kr, and Xe) and isotopic ratios, carbon isotopes ($\delta^{13}C$ and ^{14}C) and major elements. Except for He concentrations and isotopic ratios, all other results were previously published in Castro *et al.* (2012) and Warrier *et al.* (2013). He concentrations and isotopic ratios for the Saginaw aquifer are presented and discussed here for the first time. Sixteen groundwater samples were also previously collected and analyzed for all the same gases in the Marshall aquifer (Ma *et al.* 2004, 2005). Some of the previously published Marshall results are discussed here and analyzed in conjunction with the newly published He results for the Saginaw aquifer and all newly published results for the Glacial Drift aquifer.

HELIUM ISOTOPE RESULTS

Helium systematics

Excess He (He_{exc}) is calculated by removing the ASW (He_{eq}) and excess air (He_{ea}) components (Kipfer *et al.* 2002) from total measured He concentrations (He_{meas}) in groundwater samples (Stute *et al.* 1992; Castro *et al.* 2000). He_{eq} and He_{ea} are estimated based on recharge temperatures and as a function of pressure, depending on the average recharge elevation, 275 m for all three aquifers. The mean annual air temperature (MAAT) for Jackson in southeast Michigan of 9.1 ± 0.8°C (1931–2002, the MAAT data is from http://lwf.ncdc.noaa.gov/oa/climate/stationlocator.html) was adopted as the recharge temperature. He_{exc} comprises both the mantle (He_m) and crustal ($He_c = He_{cin} + He_{cext}$) components, where He_{cin} and He_{cext} are produced *in situ* within the aquifer and externally at greater depths, respectively (Castro *et al.* 2000; Ma *et al.* 2005). ^3He_t is the tritiogenic ^3He. $^3He_{exc}$ is thus given by:

$$\begin{aligned} {}^3He_{exc} &= {}^3He_{meas} - {}^3He_{eq} - {}^3He_{ea} \\ &= ({}^4He_{meas} \times R_{meas}) - ({}^4He_{eq} \times R_{eq}) - ({}^4He_{ea} \times R_{ea}) \\ &= {}^3He_{cin} + {}^3He_{cext} + {}^3He_m + {}^3He_t \end{aligned} \quad (1)$$

and

$$\begin{aligned} {}^4He_{exc} &= {}^4He_{meas} - {}^4He_{eq} - {}^4He_{ea} \\ &= {}^4He_{cin} + {}^4He_{cext} + {}^4He_m \end{aligned} \quad (2)$$

R_{eq} is the $^3He/^4He$ ratio of water in solubility equilibrium with the atmosphere, that is, $R_{eq} = 0.983 \times R_a = (1.360 \pm 0.006) \times 10^{-6}$ (Benson & Krause 1980), and R_{ea} is the $^3He/^4He$ ratio of the excess air component. Finally,

$$(R/R_a)_{exc} = ({}^3He_{exc}/{}^4He_{exc})/({}^3He_a/{}^4He_a) \quad (3)$$

where ^3He_a and ^4He_a represent the atmospheric ^3He and ^4He abundances, respectively.

The major fraction of the total ^4He excess is typically of radiogenic origin, resulting both from *in situ* production and from an external flux. These two contributions are quantified in section 'Crustal ^3He and ^4He Origin: External Versus in situ Production'. Typically, He produced in the crust results in $0.02 \leq R_c/R_a \leq 0.05$ (e.g., O'Nions & Oxburgh 1983; Castro 2004) while mantle-derived He is typically characterized by $8 \leq R_m/R_a \leq 50$ (e.g., Graham 2002; Starkey *et al.* 2009).

A typical way to separate the helium components of a groundwater sample is to plot (Weise 1986; Weise & Moser 1987):

$$\frac{^3He_{meas} - {}^3He_{ea}}{^4He_{meas} - {}^4He_{ea}} \; vs. \; \frac{^4He_{eq}}{^4He_{meas} - {}^4He_{ea}}$$

Transforming the helium balance equation according to Stute *et al.* (1992) results in a linear equation of the form $Y = a\,X + b$:

$$\underbrace{\frac{^3He_{meas} - {}^3He_{ea}}{^4He_{meas} - {}^4He_{ea}}}_{Y} = \left[R_{eq} - R_{ter} + \frac{^3He_t}{^4He_{eq}}\right] \underbrace{\frac{^4He_{eq}}{^4He_{meas} - {}^4He_{ea}}}_{X} + R_{ter} \quad (4)$$

where R_{ter} represents the $^3He/^4He$ ratio originating from terrigenic sources (crustal and mantle helium). X values vary from 0 to 1 and larger X values indicate that the ASW component is more dominant in the total He concentration and vice versa. Larger Y values mean more mantle helium or tritiogenic ^3He incorporated into the water.

If the He isotopic data from a specific aquifer represent a two-component mixture, samples plotted in the above fashion will fall along a line. However, plot results using helium data from different aquifers from around the world, including the Great Hungarian Plain (Stute *et al.* 1992) and the Carrizo aquifer (Castro *et al.* 2000; Castro 2004), clearly show that isotope data for most of the samples do not fall along a line (Castro 2004). They appear scattered and cannot record a mixture between two components. Rather, these data must reflect a mixture of three or more components, be it from *in situ* production, an external crustal origin, a mantle component, or a component of tritiogenic origin in very young groundwater.

Overall results

He concentrations and isotopic ratios, $\delta^{13}C$, ^{14}C activities and calendar ages, pH, temperature, major element data, as well as sample names, location, and well depths for the Glacial Drift and Saginaw aquifers are given in Tables 1 and 2, respectively. The Fontes & Garnier (1979) model (F&G model) ages for Saginaw samples are reported in Castro *et al.* (2012) because it utilizes both geochemical and isotopic balances to derive corrected ^{14}C ages and also to facilitate paleoclimatic comparisons with previously reported F&G corrected ^{14}C ages for samples from the Marshall aquifer (Ma *et al.* 2004). ^{14}C ages for the Glacial Drift aquifer were estimated following Mook *et al.* (1974) as opposed to the F&G model. Mook *et al.* (1974) account for initial ^{14}C values for groundwater systems that may have undergone isotopic exchange between the gaseous and aqueous carbonate systems which is characteristic of unconfined aquifers such as the Glacial Drift and is generally underestimated by the F&G model (Han & Plummer 2013). Glacial Drift and Saginaw aquifer ^{14}C ages were subsequently converted into calendar ages (cf. Section 'Sample Collection and Measurements'). Glacial Drift aquifer recharge distances were estimated by considering the distance between the locations with highest hydraulic head values in southern Michigan as given by Hoaglund *et al.* (2002) and the location of the respective samples.

For both the Glacial Drift and Saginaw aquifers, most samples display ^3He and ^4He concentrations in excess of ASW values (Table 1). These He excesses reach values of over two and three orders of magnitude above those of ASW for ^3He and ^4He, respectively, and are particularly high for samples 25, 29, 31, 62, and 65 in the Glacial Drift aquifer and samples 14, 15, and 16 in the Saginaw aquifer, located in the SL discharge area in the central portion of the basin (Fig. 3A,B). Similarly, R_{exc}/R_a values vary from 1.9 to 0.12 and from 0.830 to 0.039 for the Glacial Drift and Saginaw aquifers (Fig. 4), respectively, and are far greater for 'modern waters' as compared to older ones (Table 1).

A clear increase in ^3He (not shown) and ^4He (Fig. 3A) concentrations with recharge distance is observed in the Glacial Drift aquifer and points to the presence of strong horizontal He concentration gradients. Although the He increase with distance is smoother and more regular for the Glacial Drift aquifer than for the Saginaw aquifer, the latter exhibits a general positive exponential correlation between ^4He and recharge distance, with the exception of samples 1, 5, 6, and 12 (Fig. 3A). Overall, for most samples, He concentrations are higher in the Marshall as compared to the Saginaw aquifer which, in turn, display higher He concentrations than the Glacial Drift, pointing to increasing levels of He dilution by freshwater. A generally well-developed correlation between ^4He excesses and groundwater ages in the Saginaw aquifer is also observed (Table 2, Fig. 3B) similar to that previously observed in the Marshall aquifer (Ma *et al.* 2005). These point to a progressive accumulation of He isotopes in the Saginaw aquifer over time. However, a similar correlation in the Glacial Drift aquifer is not apparent (Table 1, Fig. 3B). This lack of correlation between He concentrations and groundwater ages in the Glacial Drift aquifer is likely due to lack of precision of ^{14}C age determination when dealing with young groundwater.

$^3H/^3He$ ages (Table 1) were calculated following Schlosser *et al.* (1988) for Glacial Drift samples gd11a, gd20a, and gd2. Samples gd20a and gd2 are modern which is consistent with subcrop recharge area samples in the Marshall and Saginaw aquifers (Ma *et al.* 2005; Castro *et al.* 2012). Tritium concentration in sample gd11a, with 0.01 TU, is beyond the $^3H/^3He$ age limit (Kazemi *et al.* 2006) and points to an age > 60 years.

This general trend of increasing excess He with recharge distance and ages is also accompanied by a progressive

Table 1 Sample Location, He Concentration, and Isotopic Ratio as well as Groundwater Age of Glacial Drift Aquifer Samples.

Sample	Recharge distance (km)	Depth (m ASL)	R/R_a	$^4He_{meas}$ (10^{-7}) (cc STP/g)	$^4He_{exc}$ (10^{-7}) (cc STP/g)	R_{exc}/R_a	Tritiogenic ^{3}He (TU)	$^3He_{exc}$ (10^{-14}) (cc STP/g) without tritiogenic ^{3}He	R_{exc}/R_a without tritiogenic ^{3}He	^{14}C Activity (%)	^{14}C Age* (yr)	±1σ	δ^{13}C (‰)	Calendar Age (yr)	^{3}H (TU)
gd02	46	−24.4	1.14 ± 0.022	0.587 ± 0.009	0.1 ± 0.026	1.9 ± 0.57	10	0.125 ± 0.404	0.09		–	–	–	–	7.64 ± 0.15
gd07a	85	−9.4	0.849 ± 0.017	0.669 ± 0.01	0.215 ± 0.03	0.57 ± 0.16	7.4	–	–		–	–	–	–	
gd11a	94	−17.4	0.913 ± 0.02	0.815 ± 0.012	0.235 ± 0.035	0.73 ± 0.2	7.4	0.526 ± 0.533	0.16		–	–	–	–	0.01 ± 0.05
gd11b	94	−17.4	1.023 ± 0.026	0.84 ± 0.013	0.214 ± 0.042	1.13 ± 0.32	13	0.091 ± 0.662	0.03		–	–	–	–	
gd18a	106	−13.7	1.162 ± 0.018	0.851 ± 0.013	0.385 ± 0.03	1.38 ± 0.14	27	0.601 ± 0.482	0.11	65.23 ± 0.22	0	0	−11.9	0	
gd18b	106	−13.7	1.178 ± 0.028	0.78 ± 0.012	0.328 ± 0.012	1.45 ± 0.09	27	–	–	65.23 ± 0.22	0	0	−11.9	0	
gd20a	113	−22.9	0.9 ± 0.016	0.457 ± 0.007	0.004 ± 0.007	–	7.4	–	–		–	–	–	–	6.00 ± 0.13
gd20b	113	−22.9	0.917 ± 0.017	0.456 ± 0.009	0.004 ± 0.009	–	7.4	–	–		–	–	–	–	
gd20c	113	−22.9	1.196 ± 0.029	0.455 ± 0.007	0.002 ± 0.007	–	7.4	–	–		–	–	–	–	
gd20d	113	−22.9	1.181 ± 0.026	0.446 ± 0.007	–	–	7.4	–	–		–	–	–	–	
gd25a	153	−12.2	0.531 ± 0.011	3.381 ± 0.051	2.827 ± 0.067	0.44 ± 0.02	40	7.294 ± 0.872	0.19	45.45 ± 0.16	0	0	−8.7	0	
gd25b	153	−12.2	0.564 ± 0.023	3.219 ± 0.048	2.623 ± 0.062	0.47 ± 0.04	40	6.994 ± 1.22	0.19	45.45 ± 0.16	0	0	−8.7	0	
gd29a	166	−11.3	0.28 ± 0.008	14 ± 0.21	13.54 ± 0.213	0.26 ± 0.01	7.4	46.09 ± 1.809	0.25	66.97 ± 0.19	2500	910	−13.5	3260	
gd29b	166	−11.3	0.385 ± 0.012	9.152 ± 0.137	8.672 ± 0.14	0.35 ± 0.02	7.4	40.38 ± 1.735	0.34	66.97 ± 0.19	2500	910	−13.5	3260	
gd31a	161	−12.2	0.241 ± 0.009	3.855 ± 0.058	3.392 ± 0.063	0.14 ± 0.01	7.4	4.709 ± 0.632	0.1	26.76 ± 0.13	4740	1740	−12.1	5270	
gd31b	161	−12.2	0.217 ± 0.007	5.261 ± 0.079	4.693 ± 0.083	0.12 ± 0.01	7.4	6.199 ± 0.656	0.1	26.76 ± 0.13	4740	1740	−12.1	5270	
gd59a	137	−15.2	0.772 ± 0.014	1.571 ± 0.024	1.09 ± 0.042	0.68 ± 0.05	7.4	8.385 ± 0.617	0.56	31.1 ± 0.14	14840	440	−15.6	17540	
gd59b	137	−15.2	0.852 ± 0.018	1.553 ± 0.023	1.055 ± 0.04	0.79 ± 0.05	7.4	9.684 ± 0.651	0.66	31.1 ± 0.14	14840	440	−15.6	17540	
gd62a	173	−14.3	0.226 ± 0.004	18.54 ± 0.278	18 ± 0.282	0.2 ± 0.01	7.4	48.71 ± 1.475	0.2	67.24 ± 0.2	6960	530	−15.1	8370	
gd62b	173	−14.3	0.401 ± 0.021	3.62 ± 0.054	3.1 ± 0.067	0.3 ± 0.03	7.4	11.16 ± 1.218	0.26	67.24 ± 0.2	6960	530	−15.1	8370	
gd65a	173	−17.4	0.179 ± 0.008	16.71 ± 0.251	16.18 ± 0.252	0.15 ± 0.01	7.4	32.24 ± 1.992	0.14	76.46 ± 0.34	5890	530	−15.8	7160	
gd65b	173	−17.4	0.182 ± 0.008	18.89 ± 0.283	18.42 ± 0.285	0.16 ± 0.01	7.4	39.39 ± 2.242	0.15	76.46 ± 0.34	5890	530	−15.8	7160	
ASW†			1	0.465											

*Calendar ages are calculated from ^{14}C ages derived from Mook model (Mook *et al.* 1974; Mook 1980).†Air-saturated water (ASW) for a temperature of 9.1°C and an altitude of 275 m (Ozima & Podosek 2002).

Table 2 Sample Location, He Concentration, and Isotopic Ratio as well as Groundwater Age of Saginaw Aquifer Samples.

Sample	Recharge distance (km)	Depth (m ASL)	R/R_a	$^4He_{meas}$ (10^{-7}) (cc STP/g)	$^4He_{exc}$ (10^{-7}) (cc STP/g)	R_{exc}/R_a	Tritiogenic ^{3}He (TU)	$^3He_{exc}$ (10^{-14}) (cc STP/g) without tritiogenic ^{3}He	R_{exc}/R_a without tritiogenic ^{3}He	^{14}C Activity (%)	^{14}C Age* (yr)	±1σ	δ^{13}C (‰)	Calendar Age* (yr)
sg01a	19	−99.1	0.299 ± 0.007	11.278 ± 0.169	10.307 ± 0.345	0.23 ± 0.03	7.4	31.489 ± 4.355	0.22	58.5 ± 0.3	0	0	−10.1	0
sg01b	19	−99.1	0.505 ± 0.016	4.013 ± 0.06	2.551 ± 0.319	0.22 ± 0.13	7.4	6.070 ± 4.439	0.17	58.5 ± 0.3	0	0	−10.1	0
sg02	28	−34.7	0.932 ± 0.01	0.943 ± 0.014	0.331 ± 0.027	0.83 ± 0.11	15	0.047 ± 0.383	0.01	86.1 ± 0.3	0	0	−11.8	0
sg03	37	−79.2	0.853 ± 0.017	0.934 ± 0.014	0.304 ± 0.055	0.57 ± 0.21	9.6	0.019 ± 0.79	0.005	43.4 ± 0.2	3600	780	−13.4	3980
sg04a	39	−61.0	0.849 ± 0.018	0.740 ± 0.011	0.118 ± 0.022	0.12 ± 0.21	7.4	–	–	51.6 ± 0.2	2730	1030	−13.8	2940
sg04b	39	−61.0	0.880 ± 0.013	0.713 ± 0.011	0.125 ± 0.018	0.38 ± 0.16	7.4	–	–	51.6 ± 0.2	2730	1030	−13.8	2940
sg05a	57	−54.9	0.186 ± 0.004	73.210 ± 1.098	72.637 ± 1.099	0.18 ± 0.01	7.4	178.794 ± 4.978	0.18	18.8 ± 0.2	9650	510	−12.6	11070
sg05b	57	−54.9	0.188 ± 0.005	66.894 ± 1.003	66.250 ± 1.004	0.18 ± 0.01	7.4	163.393 ± 5.33	0.18	18.8 ± 0.2	9650	510	−12.6	11070
sg06a	65	−67.1	0.116 ± 0.003	59.618 ± 0.894	58.962 ± 0.895	0.11	7.4	84.890 ± 2.884	0.10	46.7 ± 0.2	3700	1040	−14.1	4100
sg06b	65	−67.1	0.122 ± 0.007	54.757 ± 0.821	54.073 ± 0.825	0.11 ± 0.01	7.4	81.252 ± 5.489	0.11	46.7 ± 0.2	3700	1040	−14.1	4100
sg07	74	−61.0	0.262 ± 0.008	3.093 ± 0.046	2.463 ± 0.052	0.08 ± 0.01	7.4	0.755 ± 0.506	0.02	19 ± 0.1	11170	1090	−14.1	13060
sg08a	95	−39.6	0.106 ± 0.004	17.852 ± 0.268	17.401 ± 0.268	0.08	7.4	3.908 ± 0.743	0.05	1.2	30610	300	−10.8	35090
sg08b	95	−39.6	0.101 ± 0.004	18.390 ± 0.276	17.939 ± 0.276	0.08	7.4	6.086 ± 0.828	0.04	1.2	30610	300	−10.8	35090
sg09	96	−67.1	0.185 ± 0.006	6.230 ± 0.093	5.486 ± 0.1	0.08 ± 0.01	7.4	117.488 ± 3.911	0.18	15.1 ± 0.1	10930	230	−12.1	12820
sg10	120	−48.8	0.087 ± 0.004	128.206 ± 1.923	127.755 ± 1.923	0.08	7.4	18.202 ± 1.064	0.08	3.4 ± 0.1	22160	130	−10.9	26650
sg11	112	−85.3	0.123 ± 0.004	10.794 ± 0.162	10.032 ± 0.166	0.06 ± 0.01	7.4	17.719 ± 1.089	0.07	17.3 ± 0.1	11090	790	−13.1	12900
sg12a	53	−65.5	0.189 ± 0.005	48.94 ± 0.734	48.305 ± 0.735	0.18 ± 0.01	7.4	146.383 ± 7.466	0.08	18.7 ± 0.1	9660	450	−12.7	11080
sg12b	53	−65.5	0.19 ± 0.006	52.567 ± 0.788	52.115 ± 0.788	0.18 ± 0.01	7.4	130.241 ± 4.833	0.18	18.7 ± 0.1	9660	450	−12.7	11080
sg13	133	−97.5	0.100 ± 0.003	20.472 ± 0.307	20.021 ± 0.307	0.08	7.4	20.346 ± 0.95	0.07	0.3	42610	1170	−12.2	45940
sg14	137	−101	0.053 ± 0.004	340.472 ± 5.107	340.020 ± 5.107	0.05	7.4	241.755 ± 19.217	0.05	0.2 ± 0.1	48060	2720	−12.7	48060
sg15	155	−38.1	0.043 ± 0.005	267.727 ± 4.016	267.275 ± 4.016	0.04 ± 0.01	7.4	151.342 ± 18.68	0.04	1.4	30470	370	−11.7	35010
sg16	155	−77.7	0.054 ± 0.003	676.745 ± 10.151	676.294 ± 10.151	0.05	7.4	497.785 ± 29.105	0.05	0.4	41730	530	−11.7	45180
ASW†			1	0.465										

*^{14}C ages and calendar ages from Castro *et al.* (2012).†Air-saturated water (ASW) for a temperature of 9.1°C and an altitude of 275 m (Ozima & Podosek 2002).

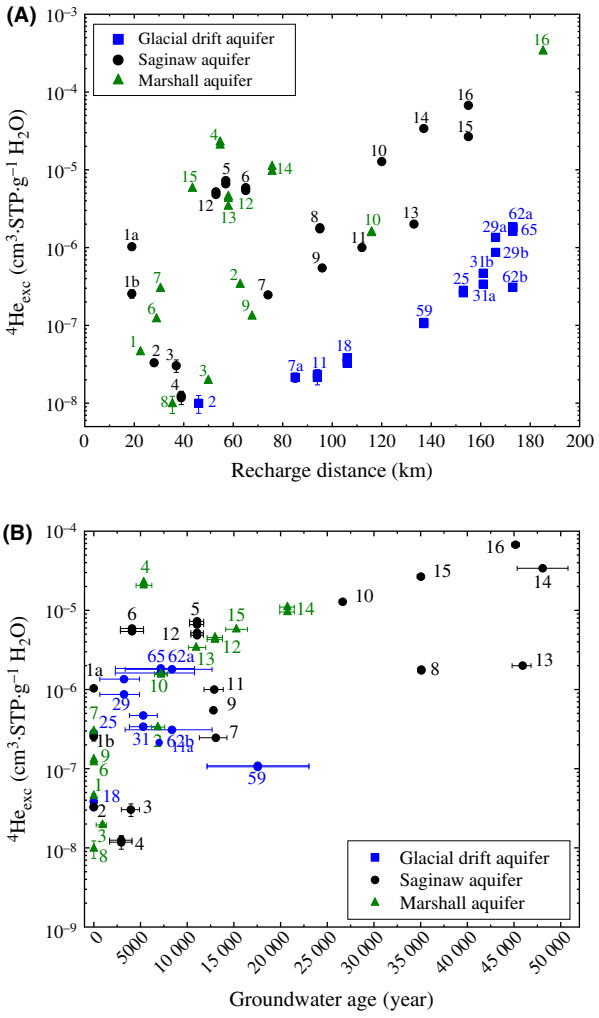

Fig. 3. ^{4}He excesses ($^4He_{exc}$) versus the recharge distance and groundwater age in the Glacial Drift, Saginaw, and Marshall aquifers. (A) Evolution of $^4He_{exc}$ concentrations in groundwater as a function of recharge distance for the Glacial Drift (blue squares, this study), Saginaw (black circles, this study), and Marshall (green triangles, Ma *et al.* 2005) aquifers; (B) ^{4}He excess versus groundwater (calendar) ages for the Glacial Drift (blue squares, this study), Saginaw (black circles, this study), and Marshall aquifers (green triangles, Ma *et al.* 2005).

evolution in water chemistry in all three aquifers. Preliminary major element analysis shows that the hydrochemical facies of the Glacial Drift, Saginaw, and Marshall aquifers evolve progressively from a CaMg-HCO_3/Na-HCO_3 facies into a NaCl facies from the recharge to the discharge areas (Table 3), reflecting the increasing impact of brines on freshwater along these groundwater flow paths. Bromide (Br^-), which behaves as a conservative element during seawater evaporation and diagenetic processes (Carpenter 1978; Stueber & Walter 1991), is considered an ideal tracer of groundwater circulation and brine sources. In the Glacial Drift and Saginaw aquifers, Br concentrations increase gradually with recharge distance (Table 1, 2, and 3) and further support the presence of upward cross-formational flow and the increasing impact of basinal brines in the central portion of the Michigan Basin and in particular, the SL area. The combined He and major element trends point unequivocally to the increased impact of cross-formational flow with increasing distance from recharge areas.

Individual helium component separation

While ^{3}He and ^{4}He present in most groundwater in sedimentary systems have a dominant crustal origin (Castro *et al.* 1998a,b, 2000), the presence of a smaller mantle component is not uncommon. In addition, $^3He_{exc}$ can result from background ^{3}H decay (7.4 TU in Michigan cf. von Buttlar & Libby 1955) or the decay of bomb ^{3}H as the nuclear bomb tests took place in the 1950s and 1960s. These three different He sources can be identified based on R_{exc}/R_a values, ^{3}He and ^{4}He excesses, as well as on groundwater age considerations (e.g., Stute *et al.* 1992; Castro 2004; Warrier *et al.* 2012). In the analysis that follows, we adopt $0.02 \leq R_c/R_a \leq 0.05$ as our 'reference' crustal value (Fig. 4). Thus, R_{exc}/R_a values greater than the latter strongly suggest the presence of a significant mantle or tritiogenic He contribution. The observed decrease in R_{exc}/R_a values in both the Glacial Drift and Saginaw aquifers is accompanied by an increase in $^3He_{exc}$ and $^4He_{exc}$ (Table 1 and 2; Fig. 4). For the Saginaw aquifer, modern groundwater samples (Table 2) display small He excesses (<10 times that of ASW values) with $0.22 \leq R_{exc}/R_a \leq 0.83$, the latter being much greater than typical crustal He values. Thus, these high R_{exc}/R_a values result from either natural or bomb ^{3}H decay or the addition of a mantle He component. As the groundwater samples become older further away from the recharge area, He excesses increase significantly, up to two and three orders of magnitude over ASW concentrations for ^{3}He and ^{4}He, respectively, with R_{exc}/R_a values approaching typical crustal values. For the Glacial Drift aquifer, although R_{exc}/R_a values for all samples are >0.05, a clear negative correlation is also observed between R_{exc}/R_a values and $^3He_{exc}$ and $^4He_{exc}$ (Table 1; Fig. 4). This observed inverse correlation between R_{exc}/R_a and $^3He_{exc}$ and $^4He_{exc}$ was also previously observed in the Marshall aquifer (Ma *et al.* 2005). This suggests that significant He excesses and, in particular, high crustal He values are found throughout the Michigan Basin in the shallowest aquifers. It further suggests some level of vertical connection and mass exchange between these three aquifers, as indicated by the similarity of their respective He isotopic signatures and decreasing excess He concentrations with decreasing depth. From the underlying Marshall aquifer to the Glacial Drift aquifer, R_{exc}/R_a values increase and point to the existence of a strong vertical R_{exc}/R_a gradient. Below, following equation (4) and section 'Helium Systematics', we estimate the contribution of

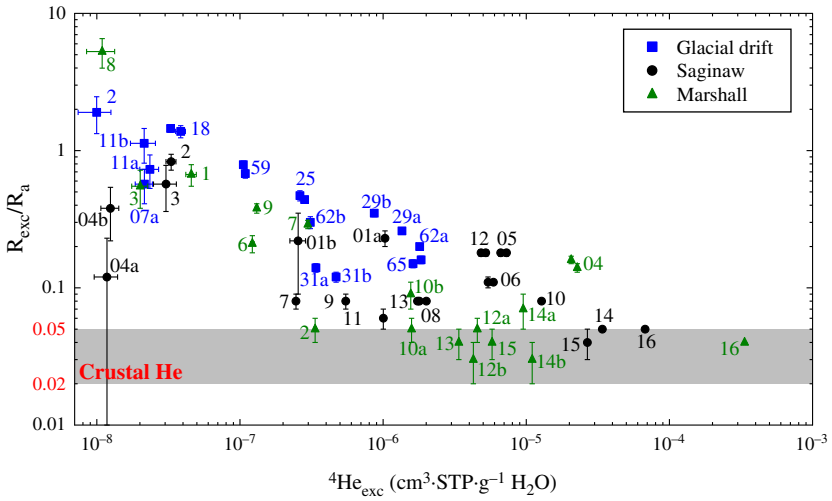

Fig. 4. R_{exc}/R_a values versus $^4He_{exc}$ concentrations for samples from the Marshall (Ma *et al.* 2005), Saginaw, and Glacial Drift aquifers, respectively. Shaded areas indicate typical crustal R/R_a values (0.02–0.05).

Table 3 Major Element Data for Samples From the Glacial Drift and Saginaw Aquifers.

Sample	pH	T (°C)	TDS (mg l^{-1})	Alkalinity (mM)	Na (mM)	K (mM)	Ca (mM)	Mg (mM)	Cl (mM)	HCO_3 (mM)	SO_4 (mM)	Br (mM)
Glacial Drift Aquifer												
gd18	7.4	11.4	320	5.900	0.452	0.038	1.984	1.334	0.100	5.723	0.466	0
gd25	6.8	11.8	1160	8.755	5.648	0.046	7.115	2.840	7.197	8.319	4.414	0
gd29	7.2	11.8	544	5.825	8.782	0.015	0.009	0.003	1.358	5.791	0.703	0.0006
gd31	7.3	11	485	4.131	7.259	0.006	0.004	0.002	0.676	4.109	0.918	0.0006
gd59	7.8	11.5	266	4.234	1.585	0.052	0.930	0.801	0.311	4.129	0.163	0.0002
gd62	7.4	11	347	6.814	0.830	0.039	2.333	1.529	0.224	6.590	0.485	0.002
gd65	7.1	11.3	817	7.051	6.387	0.055	2.917	1.743	7.329	6.823	0.498	0.002
Saginaw Aquifer*												
sg1	7.6	9.1	645	5.900	0.226	0.025	2.809	1.583	0.724	5.686	1.194	0
sg2	7.7	9.3	476	5.341	0.697	0.063	1.698	0.984	0.350	5.200	0.371	0
sg3	7.6	10.3	404	4.898	0.512	0.141	1.676	0.523	0.088	4.777	0.127	0
sg4	7.8	8	444	4.344	5.677	0.026	0.023	0.014	0.111	4.289	0.472	0
sg5	7.5	14.8	365	4.359	0.221	0.074	1.399	1.015	0.079	4.245	0.151	0
sg6	7.7	9.4	498	6.340	0.709	0.056	1.332	1.528	0.030	6.151	0.129	0
sg7	7.9	11.3	381	4.342	2.032	0.039	0.767	0.593	0.061	4.244	0.270	0
sg8	7.4	5.5	1180	3.837	7.827	0.095	3.035	1.482	5.154	3.729	4.457	0.0067
sg9	7.6	6.9	782	3.799	2.585	0.042	2.897	1.044	0.459	3.694	3.519	0
sg10	8.1	5.7	1850	3.707	25.200	0.251	0.735	0.427	20.989	3.583	2.694	0.0164
sg11	7.8	7.2	558	4.500	3.422	0.054	1.316	0.880	1.670	4.383	0.801	0.0063
sg12	7.5	14	410	4.975	0.272	0.082	1.451	0.965	0.035	4.831	0.213	0
sg13	8.3	19.8	706	4.545	9.099	0.043	0.198	0.183	2.161	4.376	1.452	0.0049
sg14	8.2	9.8	1506	5.479	21.136	0.130	0.420	0.131	15.574	5.296	1.240	0.0210
sg15	8	9.4	1510	3.384	19.093	0.198	1.248	0.575	18.216	3.264	1.612	0.0214
sg16	8	9.1	4319	3.345	67.419	0.346	2.322	1.097	63.936	3.152	1.832	0.0788

*Saginaw aquifer data from Castro *et al.* (2012).

crustal, mantle, and atmospheric He components by adopting end-member values of 0.02 for R_c/R_a (e.g., Castro 2004) and 8 for R_m/R_a (Farley & Neroda 1998), respectively.

Glacial drift aquifer

It is apparent from Fig. 5A that for most samples, the bulk of the He excess in the Glacial Drift aquifer is due to the addition of both nucleogenic ^3He and radiogenic ^4He, with R_{noea}/R_a ratios varying from 0.02 (0% mantle helium) to 0.66 (8% mantle helium) with varying contributions of tritiogenic ^3He, between 7.4 and 20 TU ^3H (1 TU = 2.5 × 10^{-15} cm^3 ^3He STP g^{-1}). Tritiogenic ^3He in the Glacial Drift aquifer likely results from both background and postbomb tritium decay. The latter is likely present in samples displaying the youngest groundwater ages (samples 2, 7, 11, 18). Assuming complete decay of 7.4 TU ^3H, 1.85 × 10^{-14} cm^3 STP g^{-1} of tritiogenic ^3He would have been added to these waters (red dashed lines, Fig. 5A). It is apparent that all samples lie

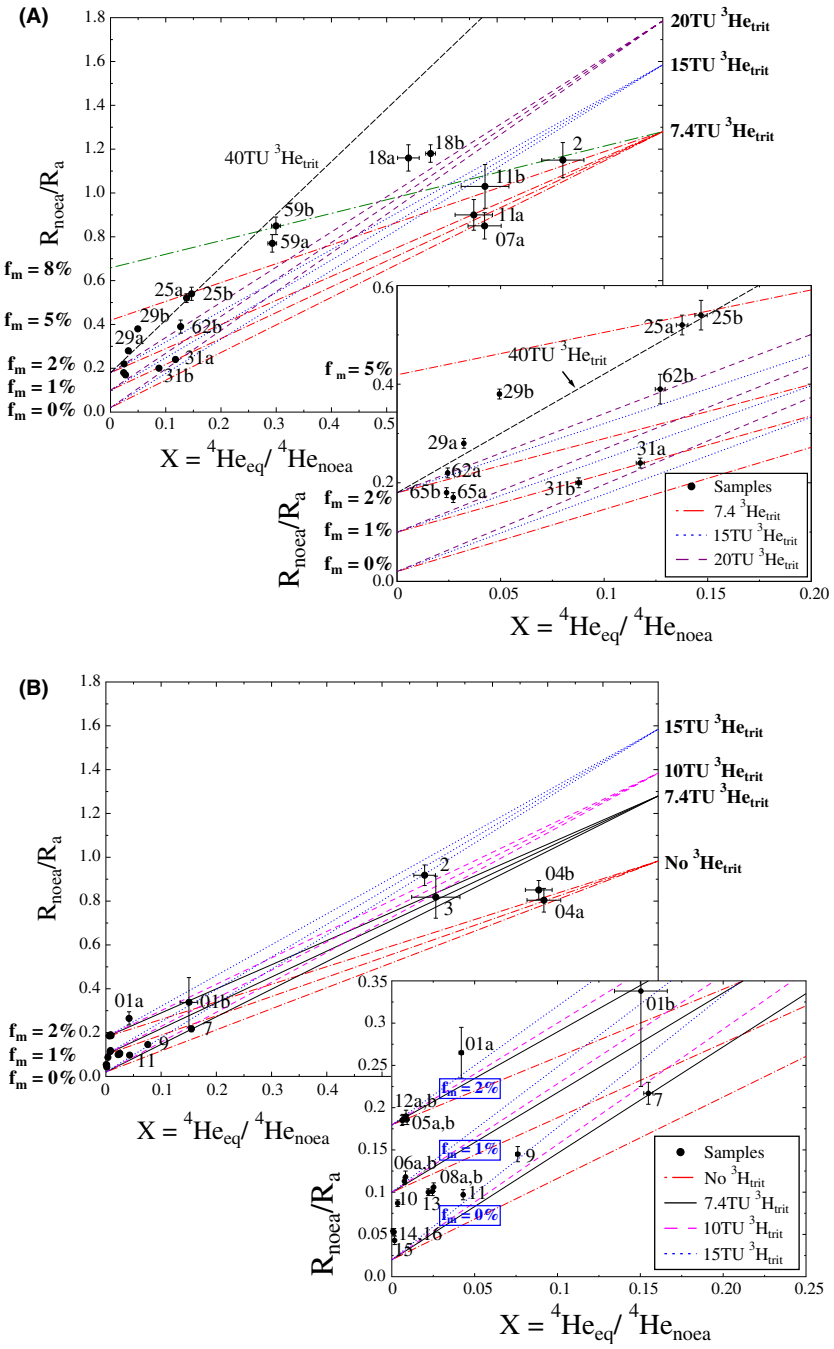

Fig. 5. R_{noea}/R_a versus $^4He_{eq}/^4He_{noea}$ for the (A) Glacial Drift and (B) Saginaw aquifers, respectively. He isotopic ratios R/R_a of the crust and the mantle are assumed to be 0.02 and 8, respectively. The prebomb background tritium concentration in this area of 7.4 TU is also indicated (Kaufman & Libby 1954; von Buttlar & Libby 1955; Thatcher 1962). Lines corresponding to 0%, 1%, 2%, 5%, and 8% mantle helium and 7.4 TU, 15 TU, and 20 TU tritiogenic He are shown for the Glacial Drift aquifer; lines corresponding to 0%, 1%, and 2% mantle helium and 0 TU, 7.4 TU, 10 TU, and 15 TU tritiogenic He are also shown for the Saginaw aquifer.

above the line corresponding to 7.4 TU tritiogenic ^{3}He with zero mantle helium contribution, pointing to either the presence of mantle He or the addition of postbomb tritiogenic ^{3}He.

$^4He_{eq}/^4He_{noea}$ of sample 25 is ~0.14, a value that is significantly lower than those of samples 2, 11, and 18, and suggests a contribution of ~2% mantle He. About 2% mantle He is estimated for sample 25 in addition to 40 TU tritiogenic ^{3}He (Fig. 5A). Sample 59 is located above the line corresponding to 7.4 TU tritiogenic ^{3}He and 5% mantle He and requires either more tritiogenic ^{3}He (~40 TU) or a higher mantle contribution (8%), of which the latter is more likely considering the fact that sample 59 is as old as 14 840 years (Table 1). This greater mantle He component in sample 59 suggests the presence of a strong upward leakage of groundwater associated with the Mid-continent Rift (MCR) System in these areas (see Figs 1 and 2) possibly carrying both 'dead' carbon and mantle He. This could also explain the observed inconsistencies in ^{14}C ages as a function of $^4He_{exc}$ and recharge distances

(Table 1, Fig. 3B). Overall, most helium in the Glacial Drift aquifer is of crustal origin, with small but non-negligible amounts of tritiogenic and mantle He components in some samples.

Saginaw aquifer

Figure 5B shows the contributions of terrigenic elements to the samples from the Saginaw Aquifer. It is apparent that nucleogenic ^{3}He and radiogenic ^{4}He also dominate the He excesses in the Saginaw samples, with R_{noea}/R_a varying between 0.02 (0% mantle helium) and 0.18 (2% mantle helium), with a tritiogenic ^{3}He contribution between 7.4 and 15 TU. The average R_{noea}/R_a value is 0.05, a value typical of crustal production. Except for sample 4, all samples for which ^{3}He/^{4}He ratios are available fall above the 7.4 TU tritiogenic ^{3}He line, indicating the existence of ^{3}He sources resulting from decay of bomb tritium and from the mantle. With the exception of samples 1a, 2, 3, 5, and 12, R_{noea}/R_a of all other samples fall between the lines corresponding to 0% and 1% mantle He contribution with 7.4 TU of possible tritiogenic ^{3}He. This confirms that the mantle helium component is small but non-negligible in the Saginaw Aquifer.

Samples 1a, 2, and 3 point to tritiogenic helium components corresponding to >20 TU, 15 TU, and 9 TU, respectively, if one assumes the fraction of mantle helium to be 0%. Samples 5 and 12 may have a helium source different from other samples with higher mantle helium contributions. This is consistent with the proximity of both samples to the MCR System (Figs 2, 3A and 5B). Sample 4 is the sole sample located below the line corresponding to 0% mantle He and 7.4 TU tritiogenic ^{3}He. However, it is possible that the tritium background has varied over time and a lower tritium background, as low as 2.5 TU, was incorporated, as opposed to the current 7.4 TU.

In a similar manner to that in the Glacial Drift aquifer, most helium in the Saginaw aquifer is of crustal origin, with smaller but non-negligible amounts of tritiogenic ^{3}He than the Glacial Drift aquifer (younger samples) and fairly minor amounts of a mantle (older samples) component.

Crustal ^{3}He and ^{4}He origin: external versus *in situ* production

From the above discussion, it is apparent that most of the ^{3}He and ^{4}He excesses in the Glacial Drift and Saginaw aquifers are of crustal origin with the addition of a small mantle component and minor tritiogenic ^{3}He. This is consistent with previous findings in the underlying Marshall aquifer (Ma *et al.* 2005). Here, we discuss the origin of the crustally produced ^{3}He and ^{4}He to ascertain whether or not $^3He_{exc}$ and $^4He_{exc}$ present in the Glacial Drift and Saginaw aquifers result mostly from *in situ* production within the aquifers, or if instead, they have a deeper external origin. With regard to the latter, it is also important to ascertain whether or not the sedimentary sequence underlying these aquifers is the main contributor or if the crystalline basement is providing most of the He excesses present in groundwater.

Production rates of ^{3}He and ^{4}He were calculated for the Glacial Drift and Saginaw aquifers and corresponding sedimentary formations underlying these aquifers, as well as the crystalline basement as follows (Ballentine 1991):

$$P(^3\mathrm{He}) = (6.035[\mathrm{U}] + 1.434[\mathrm{Th}])\times [\mathrm{Li}] \times 10^{-23}\mathrm{cm}^3\mathrm{STP}\ \mathrm{g}_{rock}^{-1}\mathrm{yr}^{-1} \quad (5)$$

$$P(^4\mathrm{He}) = 1.207 \times 10^{-13}[\mathrm{U}] + 2.867 \times 10^{-14}[\mathrm{Th}]cm^3\mathrm{STP}\ \mathrm{g}_{rock}^{-1}\mathrm{yr}^{-1} \quad (6)$$

where [Li], [U], and [Th] represent the Li, U, and Th concentrations (ppm), respectively (Table 4).

The accumulation rate of He isotopes in groundwater was then estimated according to:

$$A_{i\mathrm{He}} = P(^i\mathrm{He}) \times \rho_r \times \Lambda \times ((1-\omega)/\omega)\mathrm{cm}^3\mathrm{STP}\ \mathrm{g}_{\mathrm{H_2O}}^{-1}\mathrm{yr}^{-1} \quad (7)$$

where i represents ^{3}He or ^{4}He, ρ_r is the density of the rock in g cm^{-3}, ω is the porosity of the reservoir rock, and Λ is the transfer efficiency of He from the rock matrix to the water, assumed to be 1 (cf., Torgersen 1980; Torgersen & Clarke 1985). Table 4 lists the calculated ^{3}He and ^{4}He *in situ* production rates, thickness and porosity values for the Glacial Drift, Saginaw, and Marshall aquifers, and the sedimentary sequence underlying these aquifers in the study area. Corresponding R/R_a production values as well as ^{3}He and ^{4}He accumulation rates in groundwater for all aquifers and underlying sedimentary sequences are also indicated. ^{4}He production rates for the crystalline basement are also listed. ^{3}He production rates are not calculated for the crystalline basement due to lack of Li concentration data.

If one assumes that all ^{4}He excesses in the Glacial Drift and Saginaw groundwater result from *in situ* production, it would take between 50 and 881 kyrs, and 0.01 and 63.1 Myrs for the Glacial Drift and Saginaw aquifers, respectively, to produce the observed $^4He_{exc}$, time periods that would correspond to the required age of these groundwater samples. Such groundwater ages seem to be far too high for most samples and in contradiction with estimated ^{14}C ages (Tables 1 and 2), indicating that most of the He excess has an origin external to the aquifers. Taking into account groundwater ages as well as *in situ* production rates, the expected He accumulation in groundwater resulting solely from *in situ* production within the Glacial Drift and Saginaw aquifers is ~2–3 orders of magnitude lower than the observed He excesses

Table 4 Calculated ^{3}He and ^{4}He Production Rates and Corresponding ^{3}He/^{4}He and (R_{in}/R_a)* Ratios in the Michigan Basin as Well as *^{4}He* Production Rates in the Crystalline Basement.

Lithology	Thickness (m)	Porosity (%)	Th (ppm)	U (ppm)	Li (ppm)	Density¶ (g/cm^3)	P[^{3}He] (cm^3 STP g_{rock}^{-1} yr^{-1})	P[^{4}He] (cm^3 STP g_{rock}^{-1} yr^{-1})	^{3}He/^{4}He	R_{in}/R_a	A[^{3}He] (cm^3 STP g_{H2O}^{-1} yr^{-1})	A[^{4}He] (cm^3 STP g_{H2O}^{-1} yr^{-1})
Glacial Drift†	38	0.27	6.4	1.8	37.5	1.93	7.52E-21	4.01E-13	1.88E-08	0.014	3.92E-20	2.09E-12
Total basin thickness underneath Glacial Drift‡	2750	–	7.1	2.6	31.8	2.5	8.23E-21	5.17E-13	1.59E-08	0.011	3.11E-18	1.96E-10
Saginaw Aquifer‡	120	0.2	1.7	0.45	15	2.6	7.73E-22	1.03E-13	7.50E-09	0.005	8.04E-21	1.07E-12
Total basin thickness underneath Saginaw‡	2630	–	7.3	2.7	32.7	2.5	8.75E-21	5.35E-13	1.64E-08	0.012	2.00E-18	1.22E-10
Marshall Aquifer§	90	0.2	1.7	0.45	15	2.6	7.73E-22	1.03E-13	7.50E-09	0.005	8.04E-21	1.07E-12
Total basin thickness underneath Marshall‡	2400	–	7.4	2.7	32	2.5	8.61E-21	5.38E-13	1.60E-08	0.012	2.39E-18	1.49E-10
Crystalline Basement§	–	–	12	4	–		–	8.27E-13	–	–	–	–

*R_{in} is the helium isotopic ratio of ^{3}He/^{4}He derived from *in situ* production within the aquifer and/or corresponding sedimentary formations underneath. †U, Th, and Li estimated from average lithological composition after Parker (1967); thickness and porosity values after Olcott (1992) and Westjohn & Weaver (1998). ‡Lithological composition from Speece *et al.* (1985) and Hoaglund *et al.* (2002); U, Th, and Li estimated from average lithological composition after Parker (1967) and Tolstikhin *et al.* (1996). §From Ma *et al.* (2005). ¶Density of rocks estimated after Clark (1966).

(Fig. 6). We thus conclude that *in situ* production is a negligible He source in both, the Glacial Drift and Saginaw aquifers, compared to external contributions. Such external He sources to aquifers have been also confirmed in the Marshall aquifer (Ma *et al.* 2005). If it is assumed that all ^{3}He excesses in the Glacial Drift and Saginaw groundwater result from *in situ* production, it would take between 1.7 and 12.9 Myrs, and between 1 and 621 Myrs for the Glacial Drift and Saginaw aquifers, respectively, to produce all the ^{3}He excesses, ages which are even older than the ages calculated based on $^4He_{exc}$, and in many cases (samples 25, 29, 59, 62, and 65 in the Glacial Drift aquifer and sample 16 in the Saginaw aquifer), these are higher than the age of the formations themselves rendering it impossible for these water ages to be realistic. That suggests the ^{3}He excesses in the Glacial Drift and Saginaw aquifers have an external origin, with potentially some mantle contribution.

External sources can be provided by the underlying sedimentary sequence and/or by the crystalline basement. The sedimentary sequences underneath the Glacial Drift and Saginaw aquifers are ~2750 m and ~2630 m thick, respectively (cf., Section 'Geological and Hydrogeologic Background'; Table 4). Taking into account these different lithological compositions, thicknesses, and respective production rates, we estimate that the entire sedimentary sequence is capable of producing all $^4He_{exc}$ for some samples (e.g., samples 3, 4, 7, 9, 11 in the Saginaw aquifer and samples 31 and 59 in the Glacial Drift aquifer).

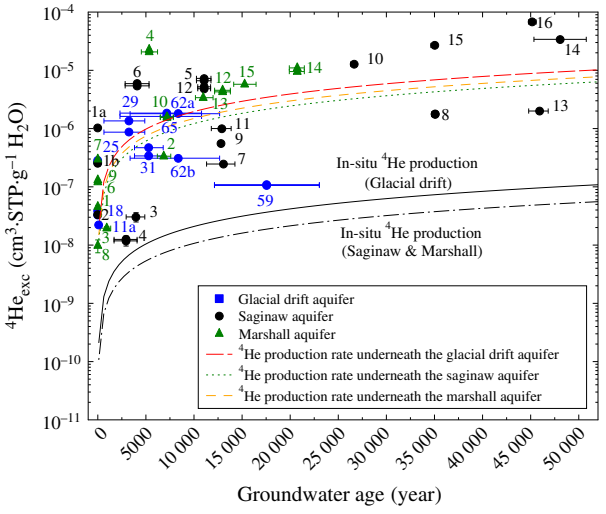

Fig. 6. ^{4}He excess versus groundwater (calendar) ages. He accumulation resulting both from in situ production in the Glacial Drift (blue squares, this study), Saginaw (black circles, this study), and Marshall aquifers (green triangles, Ma *et al.* 2005) and corresponding He concentrations resulting from production in the sedimentary sequences underneath these aquifers are also indicated for the Glacial Drift (red dashed line), Saginaw (green dashed line), and Marshall (orange dashed line) aquifers, respectively.

However, most samples in both aquifers have higher ^{4}He concentrations with respect to those that can potentially be produced in the underlying sedimentary sequences. Thus, an external He flux from deeper levels (e.g., curst and/or mantle) is required to account for these excesses (Fig. 6).

From the above discussion, it is clear that an external source dominates both $^3He_{exc}$ and $^4He_{exc}$ in both the Glacial Drift and Saginaw aquifers. In the following sections, we estimate the external vertical ^{3}He and ^{4}He fluxes entering the base of the Glacial Drift and Saginaw aquifers and further revise the previously calculated He fluxes for the Marshall aquifer (Ma *et al.* 2005) while attempting to better constrain the He sources in these aquifers.

HE TRANSPORT MODEL

Model description

In order to quantify the transfer of ^{3}He and ^{4}He to and its accumulation in a confined aquifer, Torgersen & Ivey (1985) proposed a simple model assuming that steady state for both flow and He transport is reached within the system. The advection–dispersion equation describing their model is given by:

$$v_x \frac{\partial C}{\partial x} + D_T \frac{\partial^2 C}{\partial z^2} = A \tag{8}$$

where v_x (in m yr^{-1}) is the advective pore velocity in the x (horizontal) direction, x is the distance from the recharge area of the aquifer in m, z is the relative vertical position inside the aquifer, C is the ^{3}He or ^{4}He concentration in cm^3 STP cm$^{-3}{}_{H2O}$, and D_z is the coefficient of hydrodynamic transverse dispersion in m^2 yr^{-1} given by $D_z = \alpha_T v_x + d$ (Freeze & Cherry 1977). Thus, it includes both vertical dispersion expressed as a function of transverse dispersivity (α_T) and diffusion expressed by the molecular diffusion coefficient for the solute in the porous media (longitudinal dispersive transport is neglected here as the horizontal concentration gradient is negligible as compared to the vertical one (Dagan 1989; Domenico & Schwartz 1990); A is a source term, and in our case, it represents the accumulation of ^{4}He or ^{3}He in groundwater resulting from *in situ* production as calculated from Equation (7).

It is important to note that Grasby *et al.* (2000) found that the regional-scale flow system of the Williston Basin underwent two major reversals due to the Pleistocene glaciation. Subsequently, McIntosh *et al.* (2011) confirmed also the presence of reversed groundwater flow patterns during the Pleistocene glaciation in the Michigan Basin, that is, during the LGM, at ~18 ka, primarily in the shallow glacial drift deposits. These findings suggest that transient conditions might be in place both the Williston and Michigan Basins (Grasby *et al.* 2000; Person *et al.* 2007; McIntosh *et al.* 2011). However, Hoaglund *et al.* (2002, 2004) have argued that aquifers under the Lake Michigan lobe equilibrated back to steady state relatively quickly following the retreat of the LIS. In addition and more recently, groundwater flow simulations in both steady and transient states led to the establishment of similar groundwater flow patterns in the Michigan Basin (McIntosh *et al.* 2011). Thus, following Ma *et al.* (2005), assuming steady state for both groundwater flow and He transport in the shallowest aquifer of the Michigan Basin is expected to be a reasonable assumption within uncertainties.

The prescribed boundary conditions for this model are as follows: (i) a ^{4}He or ^{3}He concentration that initially is zero for all depths in the aquifer: $[C]_{0,z} = 0$; (ii) a flux J_0 of ^{4}He or ^{3}He entering the aquifer across the bottom boundary z_o, assumed to be constant: $\left(D_z \frac{\partial C}{\partial z}\right)_{x,z0} = J_0$; and (iii) a no-flux ^{4}He or ^{3}He boundary condition at the top of the aquifer, that is, no ^{4}He or ^{3}He losses occurring through the top of the aquifer are allowed: $\left(\frac{\partial C}{\partial z}\right)_{x,0} = 0$. He studies in multilayered aquifer systems in which the advective, dispersive, and diffusive fluxes were quantified (*Castro et al.* 1998b) show a significant reduction in these ^{4}He losses of up to 30 times the total vertical flux J_0 entering at the bottom of the aquifer. In view of such results, the prescribed zero He flux boundary condition at the top of the aquifer seems to be reasonable compared to the J_0 flux entering the bottom of the aquifer (Castro *et al.* 2000).

The analytical solution to this problem is given by Torgersen & Ivey (1985):

$$C = A\frac{x}{v_x} + \frac{J_0 x}{z_0 v_x \rho} + \frac{J_0 z_0}{D_z \rho} \left[\frac{3\left(\frac{z}{z_0}\right)^2 - 1}{6} - \frac{2}{\pi^2}\sum_{m=1}^{\infty}\frac{(-1)^m}{m^2}\exp\left(-\frac{D_z m^2 \pi^2 x}{z_0^2 v_x}\right)\cos\left(\frac{m\pi z}{z_0}\right)\right] \tag{9}$$

where ρ represents the density of the groundwater.

Although the assumption of an isotropic medium does not correspond to the real situation due to, among other factors, variations in the lithology inside the same aquifer which induce variations in porosity and velocity and thus in the dispersion rate, we chose a constant value of $D_z = 0.13$ m^2 yr^{-1} for all aquifers discussed in this contribution. This choice was made on the basis of measurements of transverse dispersion performed in homogeneous sandstone at various flow rates (Freeze & Cherry 1977), showing that D_z is practically constant for a wide range of velocities (varying from 0.32 to 16 m yr^{-1}). This velocity range covers typical observations in different types of aquifers. The density value of water (ρ) was set to 1 g cm^{-3} for all aquifers and all simulations.

^{4}He and ^{3}He simulations

^{4}He and ^{3}He simulations for the Marshall aquifer were previously carried out by assuming known values for the groundwater velocity while fitting ^{4}He and ^{3}He concentrations as a function of groundwater ages (Ma *et al.* 2005). This approach led to estimated ^{3}He and ^{4}He fluxes entering the base of the Marshall aquifer of 1×10^{-13} and 1.6×10^{-6} cm^3 STP cm^{-2} yr^{-1}, respectively (Ma *et al.* 2005). Here, in addition to estimating ^{3}He and ^{4}He fluxes entering the base of the Glacial Drift and Saginaw aquifers, we also estimate ^{3}He and ^{4}He fluxes from the Marshall aquifer following a procedure similar to that used for these two other aquifers (cf. Castro *et al.* 2000).

^{4}He simulations

Velocity and water residence times are determined by fitting the ^{4}He concentrations as a function of recharge distance. The velocity v_x and the ^{4}He flux J_0 entering the base of the aquifer are the two free parameters in our model simulations. All other parameters were treated as initially known values. ^{4}He concentration distributions were obtained after fitting the model by trial and error to the measured values by numerically solving Equation (9) (10^5 terms in the series) for values of z corresponding to the bottom (z_0) and to the surface ($z = 0$ *m*) of the aquifer, respectively. Only one of the two unknown parameters (v_x and J_0) was changed at one time, that is, the simulations were conducted as if we were dealing with one variable only.

To calibrate the model, simulations were conducted as follows:

(1) We made an initial attempt to fit the ^{4}He concentrations as a function of recharge distance with a constant flux value J_0 and a constant horizontal velocity value v_x. To this end, a chosen velocity value v_x was kept constant during simulations with different values of J_0 covering five orders of magnitude. This procedure was then repeated for different velocity values, covering a range of three orders of magnitude (one order of magnitude lower and higher as compared to the previously calculated average values for these aquifers: 60 m yr^{-1} for the Glacial Drift aquifer (Long *et al.* 1988; Hall *et al.* 2012); 5.37 m yr^{-1} for the Saginaw aquifer (Mandle 1986; Hoaglund *et al.* 2002; Castro *et al.* 2012), and 2.9 m yr^{-1} for the Marshall aquifer (Mandle 1986; Hoaglund *et al.* 2002; Castro *et al.* 2012). We feel that such a procedure provides an acceptable range of v_x values for the groundwater in different types of aquifers.

The attempt to calibrate the model with both constant flux and velocity values (J_0 and v_x) failed, as it was not possible to reasonably reproduce the evolution of the observed ^{4}He concentrations as a function of distance from the recharge area. Nevertheless, these simulations made it possible to estimate, for each aquifer, an average flux value J_0 that better represents the distribution of the measured ^{4}He concentrations and that appeared to be a quasi-unique solution for each aquifer. Sensitivity tests to the flux J_0 and to the velocity v_x presented in the supplementary material provide evidence for this. The large number of sensitivity tests performed showed that only a decrease in the velocity value v_x with recharge distance x could reproduce the slope (increase) of ^{4}He concentrations with distance from the recharge area observed in each aquifer.

(2) After determining the flux value J_0 for each aquifer, the velocity remains the only unknown parameter. To determine this unknown, we first attempted to reproduce our ^{4}He concentrations with a constant velocity, followed by a linear decrease in velocity with increasing recharge distance in all aquifers. However, for all aquifers, the best fit was obtained by assuming an exponential decrease in v_x with x, where v_x is given by:

$$v_x = v_{x0} \exp\left[\log\left(\frac{v_{xf}}{v_{x0}}\right)\frac{(x - x_0)}{x_f - x_0}\right] \tag{10}$$

where x_0 is the recharge area of the aquifer; x_f is the maximum distance from the recharge area along a defined flow line in the aquifer; v_x is the horizontal velocity at a certain distance x; v_{x0} is the horizontal velocity at a distance x = v_{x0}, that is, the velocity of the groundwater in the recharge area; and v_{xf} is the velocity for $x = x_f$. Although such an exponential velocity decrease remains an assumption, such relationship has previously been observed in many aquifers around the world, including the Auob Sandstone Aquifer in Namibia and the Carrizo and Queen aquifers in Texas (Castro *et al.* 2000, 2005; Castro & Goblet 2003; Patriarche *et al.* 2004).

Equation (10) assumes that v_x becomes very small for large distances from the recharge area ($\lim_{x \to \infty} v_x = 0$). The assumption of a zero velocity for an infinite distance seems to be reasonable and corresponds to the situation observed in the discharge area itself. This assumption is reasonable, in particular, if a strong vertical leakage is present in these areas. For each aquifer, x_0 and x_f are known, with $x_0 = 0$ (recharge area) and x_f being 199 km, 160 km, and 200 km for the Glacial Drift, the Saginaw, and the Marshall aquifers, respectively. The unknown v_{x0} and v_{xf} were defined after fitting the model by iteration over a range of likely values. The velocity v_x and the time t given by $t = \int_0^x \frac{dx}{dv}$ are initially calculated for each point at a distance x, with a spatial resolution of 100 m. The calculated time value t is then integrated in Equation (9) (now expressed as a function of time) for the calculation of the ^{4}He concentrations.

^{3}He simulations

After fitting the model for ^{4}He concentrations, the velocity pattern of the aquifer is determined. With this known

velocity field for each aquifer, we have only one unknown parameter in Equation (9), that is, the ^{3}He flux J_0. It is straightforward to find out the optimal ^{3}He flux entering the bottom of the aquifer following step (2) as described above for ^{4}He.

Modeling results and discussion

Saginaw aquifer

^{4}He simulations in the Saginaw aquifer were performed for an average aquifer thickness z_o of 120 m (Vugrinovich 1986). ^{4}He and ^{3}He accumulation rates in the groundwater (source term in Equation 9) were taken as 1.07×10^{-12} and 8.04×10^{-21} cm^3 STP cm$^{-3}{}_{H2O}$ yr^{-1}, respectively (Table 4). Following the calibration procedure described in the previous section, sensitivity tests for a constant flux (J_0) and velocity (v_x) values were performed covering 5 orders of magnitude of He flux values, from 6.1×10^{-5} to 6.1×10^{-9} cm^3 STP cm^{-2} yr^{-1} and for velocity values one order of magnitude lower and higher, respectively (0.537 and 53.7 m yr^{-1}), than the average velocity value previously used (Castro *et al.* 2012; Text S1). Sensitivity tests showed that the flux value J_0 entering the bottom of the aquifer is to a large extent independent of the horizontal velocity of the groundwater and thus represents a 'quasi-unique' solution. Sensitivity results also showed that to reproduce the increase in ^{4}He concentrations as well as a reduction in the ^{4}He gradient between the top and bottom of the aquifer toward the discharge area, the velocities of the groundwater have to be decreased with increasing recharge distance.

Figure 7A and B show the simulated $^4He_{exc}$ and $^3He_{exc}$ from the bottom ($z = 120$ *m*) and top of the Saginaw aquifer ($z = 0$ m) as a function of the recharge distance for our calibrated model. Contributions of $^3He_{exc}$ and $^4He_{exc}$ from *in situ* accumulation in the groundwater are also shown (lower dashed lines). Simulated $^4He_{exc}$ and $^3He_{exc}$ reproduce reasonably well both the increase in measured He excesses and the decrease in excess range values with increased recharge distance. With the exception of samples 14, 15, and 16 for ^{4}He simulations and samples 5, 12, 14, and 16 for ^{3}He, most measured concentrations fall within simulated values between the bottom and the top of the aquifer.

The optimal fit obtained indicates that He excesses in the Saginaw aquifer require external He flux values of 7.5×10^{-14} and 6.1×10^{-7} cm^3 STP cm^{-2} yr^{-1} for ^{3}He and ^{4}He, respectively (Fig. 7A,B). Estimated He fluxes yield a $R_{exc}/R_a = 0.089$ entering the bottom of the Saginaw aquifer, a value that is very close to the observed average R_{exc}/R_a of 0.09 if one excludes the tritiogenic ^{3}He contributions (Table 1, Fig. 7A,B) which is not considered in our simulations. The model also suggests, as previously concluded, that *in situ* production from the Saginaw aquifer is negligible, yielding concentrations that are 3–5 orders of magnitude lower than the observed ^{3}He and ^{4}He excesses in the Saginaw aquifer (Fig. 7A,B).

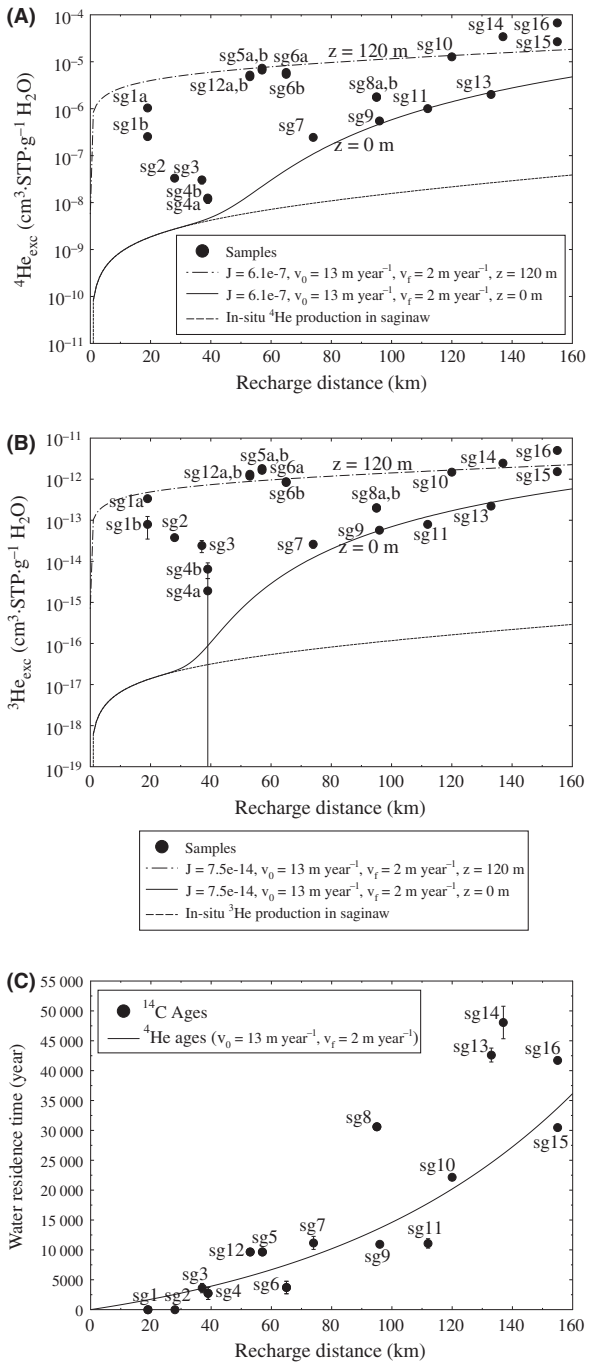

Fig. 7. Calculated (A) $^4He_{exc}$ and (B) $^3He_{exc}$ concentrations for the bottom (z = 120 m) and for the top of the aquifer (z = 0 m) as a function of the recharge distance for the Saginaw aquifer. Measured $^4He_{exc}$ and $^3He_{exc}$ concentration values are also shown as well as the ^{4}He and ^{3}He concentration curves resulting from in situ production only (lower dashed line). (C) Calculated groundwater residence times for the Saginaw aquifer using $^4He_{exc}$ distribution concentrations (this study) and ^{14}C measurements (Castro *et al.* 2012) as a function of recharge distance.

Such high fluxes entering the bottom of the Saginaw aquifer cannot explain the high $^4He_{exc}$ of samples 14, 15, and 16, nor the high $^3He_{exc}$ of samples 5, 12, 14, and 16. Fitting observed He excesses for these samples requires fluxes that are far greater than the estimated average ^{3}He and ^{4}He fluxes (Table 5). Specifically, for samples 5 and 12, ^{3}He fluxes of 1.42×10^{-13} and 1.07×10^{-13} cm^3 STP cm^{-2} yr^{-1} are required, resulting in simulated R_{exc}/R_a values of 0.17 and 0.13, respectively. The latter are consistent with measured R_{exc}/R_a values without tritiogenic ^{3}He of 0.18 and 0.13 for samples 5 and 12, respectively (cf. Table 2). This, in turn, points to the presence of a more significant mantle He component in these two samples. As previously suggested, it is likely that the presence of faults in this area (Fig. 2) may act as conduits for groundwater from greater depths, and from the crystalline basement in particular, thereby enhancing vertical He transport. To fit ^{4}He excesses for samples 14, 15, and 16, ^{4}He fluxes between 8.9×10^{-7} and 2.2×10^{-6} cm^3 STP cm^{-2} yr^{-1} are required. For $^3He_{exc}$, flux values of 8.9×10^{-14} and 1.67×10^{-13} cm^3 STP cm^{-2} yr^{-1} are required for samples 14 and 16, respectively. These yield R_{exc}/R_a of 0.05, 0.06, and 0.05 for samples 14, 15, and 16, respectively. In a manner similar to that of samples 5 and 12, simulated R_{exc}/R_a are consistent with measured R_{exc}/R_a without tritiogenic ^{3}He for these samples (Tables 2 and 4) and present a much higher crustal He component than samples 5 and 12. This lower simulated R_{exc}/R_a and higher ^{3}He and ^{4}He fluxes point to the presence of upward groundwater flow in the Saginaw Lowland as previously indicated by Mandle & Westjohn (1989) and Hoaglund *et al.* (2004).

Significantly higher fluxes than average at certain locations in the Saginaw and also in the Marshall aquifer (cf. section 'Marshall aquifer') strongly suggest the presence of vertical pathways (Seal Bypass Systems—SBS, Cartwright *et al.* 2007) within the central portion of the Michigan Basin. These Seal Bypass Systems in the central portion of the Michigan Basin might also impair their potential as nuclear waste repositories. However, Ordovician shales and carbonates on the eastern flank of the Michigan Basin were recently found to be well isolated from overlying formations (Clark *et al.* 2013), thus considerably strengthening the safety of nuclear waste disposal in this geological repository. These discrepancies between central and eastern Michigan Basin reflect the heterogeneity of deep Michigan Basin formations.

Despite the uncertainty associated with these calculations, it is clear that He fluxes entering the Saginaw aquifer are far greater than He fluxes reported in other sedimentary basins at similar (≤300 m), and even far greater depths (Fig. 8). For example, the upward ^{4}He flux entering the Saginaw aquifer is over an order of magnitude greater than the one entering the Carrizo aquifer in the Gulf Coast Basin (average depth 1000 m; Castro & Goblet 2003; Patriarche *et al.* 2004) and presents an intermediate value between fluxes entering the Albian (depth ~600 m) and Lusitanian aquifers (depth ~1600 m) at the center of the Paris Basin (Castro *et al.* 1998b). A similar pattern is observed for ^{3}He fluxes. Such high He fluxes present at such shallow depths strongly suggest that a dominant vertical flow component (upward leakage) with respect to a horizontal one is present within the Michigan Basin and the impact of the horizontal flow component at depth is minor (Ma *et al.* 2005).

Concerning the Saginaw aquifer velocity field, the best fit for He concentrations' distribution as a function of recharge distance was obtained for an exponential velocity

Table 5 Comparison of R_{exc}/R_a Modeling and Measured Results for Specific Samples in the Saginaw and Marshall Aquifers.

Samples	Modeling ^{3} He flux	Modeling ^{4} He flux	Modeling R_{exc}/R_a of the flux	Measured R_{exc}/R_a without tritiogenic ^{3}He
Saginaw Aquifer				
sg05	1.42E-13	6.10E-07	0.17	0.18
sg12	1.07E-13	6.10E-07	0.13	0.13
sg14	8.90E-14	1.30E-06	0.05	0.05
sg15	7.50E-14	8.90E-07	0.06	0.04
sg16	1.67E-13	2.20E-06	0.05	0.05
Marshall Aquifer				
mr04	4.80E-13	2.30E-06	0.15	0.15
mr16	7.70E-13	1.50E-05	0.04	0.04

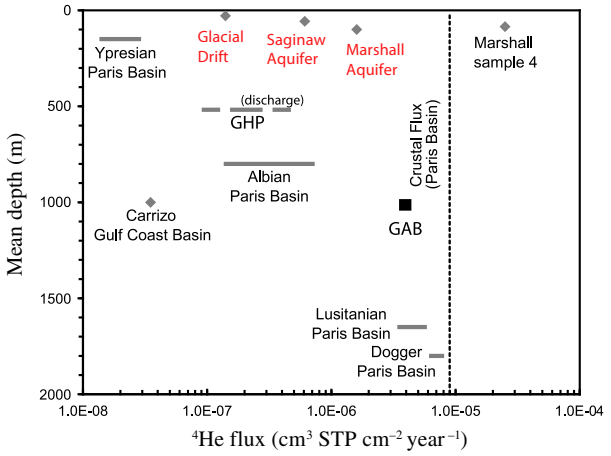

Fig. 8. Estimated ^{4}He fluxes entering the Marshall, Saginaw, and Glacial Drift aquifers (this study), respectively. ^{4}He fluxes entering aquifers in other multilayered sedimentary basins are also indicated. These include the Carrizo aquifer in the Gulf Coast Basin (Castro & Goblet 2003), the Ypresian, Albian, Lusitanian, and Dogger aquifers in the central portion of the Paris Basin (Castro *et al.* 1998b), and the Great Artesian Basin (Torgersen & Ivey 1985). Although not a multilayered system, ^{4}He fluxes estimated in the Great Hungarian Plain (Stute *et al.* 1992) are also indicated for comparison; the crustal flux entering the Paris Basin is also indicated (Castro *et al.* 1998b).

decrease between the recharge and discharge areas from $v_0 = 13$ m yr^{-1} to $v_f = 2$ m yr^{-1}. This velocity range is consistent with results obtained through pumping tests (Mandle & Westjohn 1989) and groundwater flow modeling (Hoaglund *et al.* 2002). This reduction in the velocity field toward the discharge area is also in agreement with the observed decrease in hydraulic gradient (Fig. 2; Westjohn & Weaver 1996b; Hoaglund *et al.* 2002) and consistent with the occurrence of upward water leakage as discussed earlier in section 'Helium Isotope Results'.

First-order approximation groundwater residence times estimated from ^{4}He simulations are plotted as a function of recharge distance together with previously estimated ^{14}C ages (Fig. 7C, Castro *et al.* 2012). From this figure, it is apparent that from the recharge to the discharge area, ^{4}He ages increase gradually from modern to around 32 500 years, while ^{14}C ages vary from modern to 48 060 years (sample 14, see also Table 2) with some exceptions. Overall, mean estimated ^{4}He groundwater residence times follow a pattern similar to that of ^{14}C ages and both ages correlate reasonably well. Exceptions to this general observation are samples 8, 13, 14, and 16 displaying significantly older ^{14}C ages. As previously discussed for the Carrizo aquifer (e.g., Castro *et al.* 2000; Castro & Goblet 2005), ^{14}C ages can be the result of a local situation in a particular area, contrary to the ^{4}He ages corresponding to an average age of the water, thus giving origin to some discrepancies. It is important to note that the currently estimated ^{4}He ages using this analytical, highly simplified model are first-order approximation water ages and do not reflect local hydrodynamic and structural features which might be present and which might be better revealed by ^{14}C ages (see, e.g., Castro & Goblet 2005) and by ^{4}He ages when carrying out more complex and detailed numerical modeling simulations of coupled groundwater flow and He transport (e.g., Patriarche *et al.* 2004; Castro *et al.* 2007).

Marshall aquifer

Figure 9A and B show the calculated curves for the bottom ($z = 90$ m) and top of the aquifer ($z = 0$ m) as a function of recharge distance, as well as the measured $^4He_{exc}$ and $^3He_{exc}$ concentrations. Contributions of *in situ* produced ^{4}He and ^{3}He to groundwater are also shown. Simulated external He flux values in the Marshall aquifer are 1×10^{-13} and 1.6×10^{-6} cm^3 STP cm^{-2} yr^{-1} for ^{3}He and ^{4}He, respectively, and reproduce the measured range in He concentrations with the exception of samples 4 and 16 (Fig. 9A,B). High ^{4}He and ^{3}He concentrations for these two samples are likely due to groundwater mixing between the Marshall aquifer and that of upward cross-formational flow with higher He concentrations (Ma *et al.* 2005). Values for ^{4}He and ^{3}He best fitting concentrations for samples 4 and 16 (Table 5) yield R_{exc}/R_a of 0.15 and 0.04, respectively, values that are consistent with measured R_{exc}/R_a without tritiogenic ^{3}He, strongly suggesting the presence of a more significant mantle component in sample 4 and an even more dominant crustal component in sample 16, the latter likely due to strong upward cross-formational flow in the major discharge area of the Michigan Basin.

Model calibration was obtained for an exponential decrease in the velocity v_x from 18 to 6 m yr^{-1} from the recharge to the discharge area, an average velocity that is higher than that of the overlying Saginaw aquifer. Although this is somewhat surprising, it is consistent with hydraulic conductivities derived from multiple aquifer tests performed in the area, in particular, in an area extending from Battle Creek to the center of the basin, which yield values ranging from 5×10^{-7} to 1.94×10^{-3} m s^{-1} (Mandle & Westjohn 1989). Using hydraulic head values given by Hoaglund *et al.* (2002), an average hydraulic gradient value of 1.1×10^{-3} is estimated. From these, assuming the Marshall to be isotropic, water velocities ranging between 0.02 and 67 m yr^{-1} are derived. This estimated range of velocity values is consistent with our calibrated model results. Although our model is capable of reproducing measured He concentrations for both ^{4}He and ^{3}He in the Marshall aquifer, corresponding ^{4}He ages which increase gradually from modern to around 14 240 years ($x = 160$ km) from the recharge to the discharge areas have no significant correlation with ^{14}C ages, which, with the exception of samples 2, 4, and 12–15 increase from modern to 6380 years (sample 10) along the flow path (Fig. 9C, Ma *et al.* 2004). In particular, ^{14}C ages of Marshall samples display poor correlation with recharge distance (Fig. 9C). This can be due to the fact that most of our samples, which are located relatively close to the recharge area, fall along different flow paths. This unbalanced sample location between the recharge and discharge areas might also be contributing to a bias toward an overestimation of water velocities through He simulations. As pointed out previously for the Saginaw aquifer, however, these ^{4}He ages are first-order approximation ages and unable to reproduce in detail hydrodynamic and structural features in this aquifer. Therefore, discrepancies between ^{14}C and ^{4}He ages are expected. In the near future, we expect to build a more detailed and complex numerical model to conduct both simulations of groundwater flow and He transport and thus use He as a tool to derive far more precise groundwater residence times.

Glacial drift aquifer

The Glacial Drift aquifer is the shallowest, unconfined aquifer in the Michigan Basin, which overlies the Saginaw aquifer. Our model simulations indicate that measured ^{3}He and ^{4}He concentrations in the Glacial Drift aquifer require He flux values entering the base of the aquifer of 5.2×10^{-14} and 1.5×10^{-7} cm^3 STP cm^{-2} yr^{-1} for ^{3}He

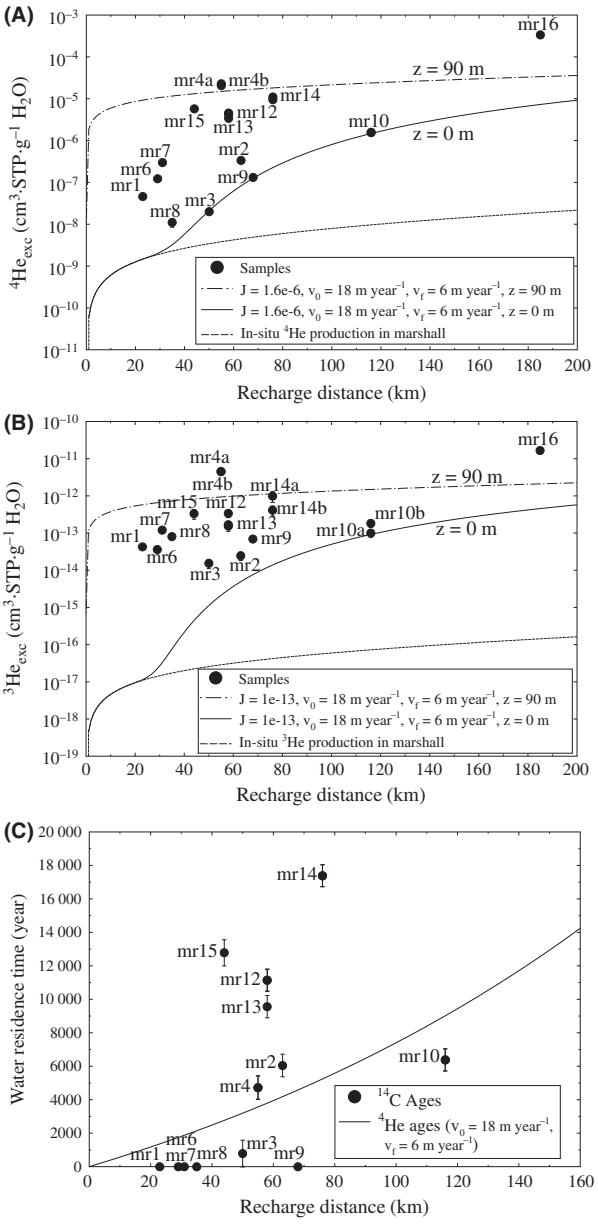

Fig. 9. Calculated (A) $^4He_{exc}$ and (B) $^3He_{exc}$ concentration curves for the bottom (z = 90 m) and the top of the aquifer (z = 0 m) as a function of recharge distance for the Marshall aquifer. Measured $^4He_{exc}$ and $^3He_{exc}$ concentration values are also shown as well as the ^{4}He and ^{3}He concentration curves resulting from in situ production only (lower dashed line). (C) Calculated groundwater residence times for the Marshall aquifer using $^4He_{exc}$ distribution concentrations (this study) and ^{14}C measurements (Ma *et al.* 2004, 2005) as a function of recharge distance.

and ^{4}He, respectively (Fig. 10A,B), values which are lower than the He flux values obtained for the Saginaw and Marshall aquifers (Fig. 8). These flux values are capable of reproducing the measured He concentrations with the exception of samples 62 for both ^{3}He and ^{4}He, 59 for ^{4}He, and 31 for ^{3}He for which concentrations are slightly underestimated.

Estimated He fluxes correspond to a R_{exc}/R_a value of 0.25, a value that is in agreement with the observed average measured R_{exc}/R_a without tritiogenic ^{3}He value of 0.22 for all samples (Table 1, Fig. 10A,B). This simulated Glacial Drift R_{exc}/R_a value is higher than that of the Saginaw aquifer, which, in turn, is higher than that of the Marshall aquifer. This increasing trend in R_{exc}/R_a from the deeper Marshall to the shallower Glacial Drift aquifer suggests a decreasing dominance of crustal He, together with increased dilution of He concentrations by freshwater and possibly, an increase in tritiogenic ^{3}He. Conversely, from the lower Marshall aquifer to the upper Glacial Drift aquifer, simulated He fluxes for ^{3}He and ^{4}He, respectively, point also to an increased impact of recharge water on crustal He being carried through upward cross-formational flow. Measured relatively low He concentrations in samples 59 and 62 are accompanied by older ^{14}C ages (Fig. 10A, C) and suggest a lower local *in situ* He production rate, which occurs in an area that is locally much less permeable than the rest of the formation (also revealed by the well logs of these sampled wells; see also Westjohn *et al.* 1994) and where groundwater could be isolated from the general circulation and thus much older (Castro *et al.* 2000).

This model is fitted for velocity values v_x decreasing exponentially from 250 to 5 m yr^{-1} from the recharge toward the discharge area, that is, from areas with highest hydraulic head values in southwest Michigan to the regional Michigan Basin discharge area in the Saginaw Lowlands (Hoaglund *et al.* 2002). This range of velocity values is consistent with previous findings (Long *et al.* 1988; Cypher & Lemke 2009). Figure 10C shows that estimated water ages in the Glacial Drift aquifer through both ^{14}C and ^{4}He are at present highly uncertain. ^{14}C ages in the Glacial Drift aquifer vary from modern (samples gd18 and gd25) to 148 40 years (sample gd59) and, with the exception of gd59, they display an overall pattern of increasing ages with increased recharge distance. This increase in ^{14}C ages with greater recharge distance is also observed for ^{4}He ages, which vary from modern to about 5800 years (gd65; Fig. 10C). The unconfined nature of the Glacial Drift aquifer renders age estimation more complex as compared to confined aquifers and further work to better constrain the Glacial Drift water ages will be undertaken in the future.

CONCLUSIONS

We present helium and major ion data for the Saginaw and Glacial Drift aquifers in the Michigan Basin, in addition to ^{14}C and tritium data for some samples in the Glacial Drift. These two shallow groundwater data sets are subsequently interpreted in conjunction with helium, ^{14}C and major element data from the deeper Marshall aquifer previously analyzed (Ma *et al.* 2005).

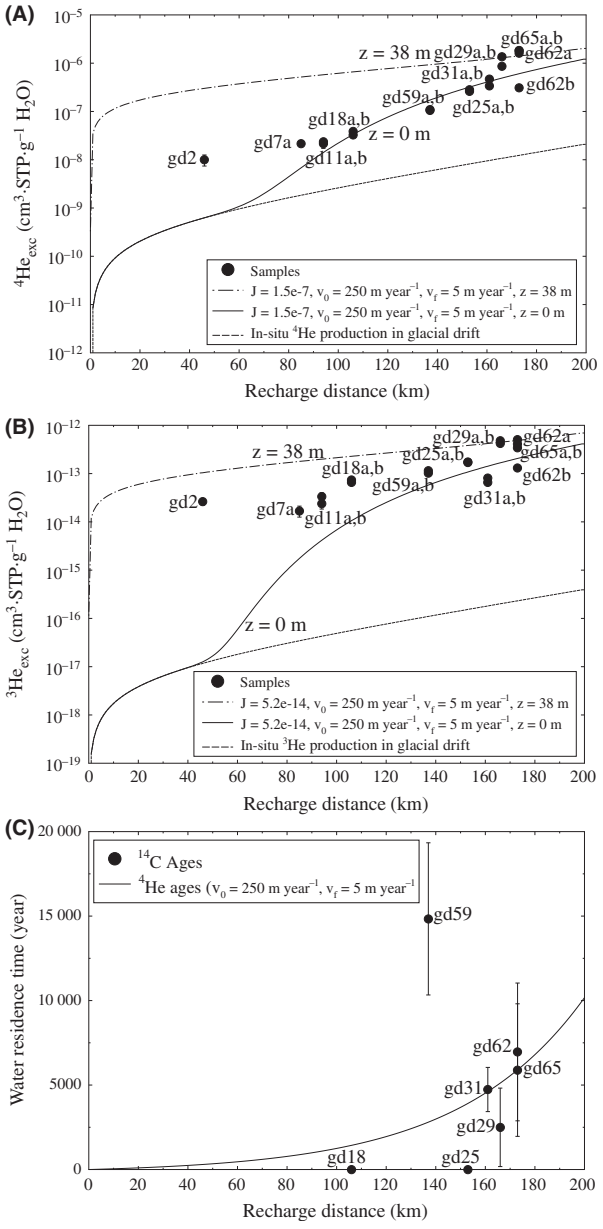

Fig. 10. Calculated (A) $^4He_{exc}$ and (B) $^3He_{exc}$ concentration curves for the bottom (z = 38 m) and for the top of the aquifer (z = 0 m) as a function of the recharge distance for the Glacial Drift aquifer. Measured $^4He_{exc}$ and $^3He_{exc}$ concentration values are also shown as well as the ^4He and ^3He concentration curves resulting from in situ production only (lower dashed line). (C) Calculated groundwater residence times for the Glacial Drift aquifer using $^4He_{exc}$ distribution concentrations and ^{14}C measurements (this study) as a function of recharge distance.

For all three aquifers, He excesses are unusually high for such shallow depths and suggest the presence of a dominant crustal He component (nucleogenic ^3He and radiogenic ^4He) in most groundwater samples with the presence of a non-negligible mantle He component in some of the samples. Such high He excesses in the Glacial Drift and Saginaw aquifers require a He source external to these two aquifers, which is consistent with previous findings in the Marshall aquifer (Ma *et al.* 2005). The transition from CaMg-HCO_3/Na-HCO_3 facies to NaCl facies from the recharge to the discharge area in all three aquifers and increasing trend of Br concentrations with recharge distances in the Glacial Drift and Saginaw aquifers also support this finding. In addition to some mantle He, this external He flux can be supplied by underlying formations within the sedimentary sequence in addition to the crystalline basement. Some tritiogenic ^3He is also found in the youngest groundwaters.

To estimate the ^3He and ^4He fluxes entering the base of the Glacial Drift, the Saginaw and the Marshall aquifers, a modified version of the analytical model developed by Torgersen & Ivey (1985), was applied. Results show that ^3He and ^4He fluxes entering the bottom of the Saginaw aquifer are 7.5×10^{-14} and 6.1×10^{-7} cm^3 *STP* cm^{-2} yr^{-1}, both of which are lower than the flux values entering the Marshall aquifer, 1×10^{-13} and 1.6×10^{-6} cm^3 STP cm^{-2} yr^{-1} for ^3He and ^4He, respectively. On the other hand, He flux values entering the Saginaw aquifer are higher than the He fluxes entering the Glacial Drift aquifer of 5.2×10^{-14} and 1.5×10^{-7} cm^3 STP cm^{-2} yr^{-1} for ^3He and ^4He, respectively. ^3He and ^4He fluxes in these three aquifers are unusually high at such shallow depth and are one to two orders of magnitude greater than those entering the deeper Carrizo aquifer in the Gulf Coast Basin and comparable to those in the deeper aquifers of Paris Basin and the Great Artesian Basin (Fig. 8). Furthermore, the He fluxes are decreasing from the lower Marshall aquifer to the upper Glacial Drift aquifer (Fig. 8) which strongly suggests the presence of a dominant vertical groundwater flow component, that is, the presence of upward cross-formational flow, with increasing He dilution with decreasing depth by horizontal flow of meteoric water entering recharge areas. Helium transport simulations also suggest that the contribution of *in situ* ^3He and ^4He production to measured He concentrations in all three aquifers is negligible, being two to five orders of magnitude lower with respect to contribution from external He sources.

Model simulations suggest that an exponential decrease in the groundwater velocity with increasing recharge distance from the recharge area is required to explain the distribution of the observed ^3He and ^4He concentrations in all three aquifers. These velocity values vary from 13 to 2 m yr^{-1} for the Saginaw aquifer and from 18 to 6 m yr^{-1} for the Marshall aquifer, between the recharge and discharge areas, respectively. The Glacial Drift aquifer displays a greater range in velocity values, with a decrease from the recharge toward the discharge areas from 250 to 5 m yr^{-1}. The exponential decrease in horizontal flow velocity in these three aquifers is also consistent with the presence of leakage in this system. Based on their known velocity

fields, ^{4}He ages were estimated for the Glacial Drift, the Saginaw, and the Marshall aquifers. While Saginaw ^{4}He ages display an overall agreement with ^{14}C ages (Castro *et al.* 2012), ^{14}C and ^{4}He ages in the Glacial Drift and Marshall aquifers deviate significantly, possibly due to the high uncertainties in ^{14}C ages in the Glacial Drift aquifer which display, modern ages for most of the samples. In addition, He ages calculated through this analytical model are first-order approximation ages due to the simplifications introduced in the model and are thus not expected to be able to reproduce certain hydrodynamic and geologic features in these aquifers which might significantly impact the water ages.

ACKNOWLEDGEMENTS

We thank Prof. Mark Person for the editorial handling of this manuscript as well as two anonymous reviewers for their insightful and thorough reviews. We also thank all homeowners for access to their wells. Financial support by the National Science Foundation CAREER award EAR-0545071 is greatly appreciated.

REFERENCES

Ballentine CJ (1991) *He, Ne, and Ar Isotopes as Tracers in Crustal Fluids*. Cambridge University Press, Cambridge, England.

Ballentine CJ, Hall CM (1999) Determining paleotemperature and other variables by using an error-weighted, nonlinear inversion of noble gas concentrations in water. *Geochimica et Cosmochimica Acta*, **63**, 2315–36.

Barton GJ, Mandle RJ, Baltusis MA (1996) Predevelopment freshwater heads in the glaciofluvial, Saginaw, and Marshall aquifers in the Michigan Basin, Open- File Report. U.S. Geological Survey, Branch of Information Services [distributor], pp. iv, 15 pp., Illinois, maps, 28 cm.

Benson B, Krause D Jr (1980) Isotopic fractionation of helium during solution: a probe for the liquid state. *Journal of Solution Chemistry*, **9**, 895–909.

von Buttlar H, Libby WF (1955) Natural distribution of cosmic-ray produced tritium II. *Journal of Inorganic and Nuclear Chemistry*, **1**, 75–91.

Carpenter AB (1978) Origin and chemical evolution of brines in sedimentary basins. *Oklahoma Geological Survey Circular*, **79**, 60–77.

Cartwright J, Huuse M, Aplin A (2007) Seal bypass systems. *AAPG Bulletin*, **91**, 1141–66.

Castro MC (2004) Helium sources in passive margin aquifers—new evidence for a significant mantle ^{3}He source in aquifers with unexpectedly low in-situ ^{3}He/^{4}He production. *Earth and Planetary Science Letters*, **222**, 897–913.

Castro MC, Goblet P (2003) Calibration of regional groundwater flow models: working toward a better understanding of site-specific systems. *Water Resources Research*, **39**, 1172–96.

Castro MC, Goblet P (2005) Calculation of ground water ages—a comparative analysis. *Ground Water*, **43**, 368–80.

Castro MC, Hall CM, Patriarche D, Goblet P, Ellis BR (2007) A new noble gas paleoclimate record in Texas — Basic assumptions revisited. *Earth and Planetary Science Letters*, **257**, 170–87.

Castro MC, Jambon A, de Marsily G, Schlosser P (1998a) Noble gases as natural tracers of water circulation in the Paris Basin: 1. Measurements and discussion of their origin and mechanisms of vertical transport in the basin. *Water Resources Research*, **34**, 2443–66.

Castro MC, Goblet P, Ledoux E, Violette S, de Marsily G (1998b) Noble gases as natural tracers of water circulation in the Paris Basin: 2. Calibration of a groundwater flow model using noble gas isotope data. *Water Resources Research*, **34**, 2467–83.

Castro MC, Stute M, Schlosser P (2000) Comparison of ^{4}He ages and ^{14}C ages in simple aquifer systems: implications for groundwater flow and chronologies. *Applied Geochemistry*, **15**, 1137–67.

Castro MC, Patriarche D, Goblet P (2005) 2-D numerical simulations of groundwater flow, heat transfer and ^{4}He transport—implications for the He terrestrial budget and the mantle helium–heat imbalance. *Earth and Planetary Science Letters*, **237**, 893–910.

Castro MC, Ma L, Hall CM (2009) A primordial, solar He-Ne signature in crustal fluids of a stable continental region. *Earth and Planetary Science Letters*, **279**, 174–84.

Castro MC, Warrier RB, Hall CM, Lohmann KC (2012) A late Pleistocene-Mid-Holocene noble gas and stable isotope climate and subglacial record in southern Michigan. *Geophysical research letters*, **39**, L19709.

Catacosinos AP, Daniels PAJ (1991) Stratigraphy of middle Proterozoic to Middle Ordovician formations of the Michigan basin. *Geological Society of America Special Paper*, **256**, 53–71.

Clark SP (1966) *Handbook of Physical Constants*. Geological Society of America, New York.

Clark ID, Al T, Jensen M, Kennell L, Mazurek M, Mohapatra R, Raven KG (2013) Paleozoic-aged brine and authigenic helium preserved in an Ordovician shale aquiclude. *Geology*, **41**, 951–4.

Cypher JA, Lemke LD (2009) Multiple working transport hypotheses in a heterogeneous glacial aquifer system. *Ground Water Monitoring & Remediation*, **29**, 105–19.

Dagan G (1989) *Flow and Transport in Porous Formations*. Springer, Berlin, Heidelberg.

Domenico PA, Schwartz FW (1990) *Physical and Chemical Hydrogeology*. John Wiley & Sons, Chichester, England.

Dorr JAJ, Eschman DF (1970) *Geology of Michigan*. University of Michigan, Ann Arbor.

Farley KA, Neroda E (1998) Noble gases in the earth's mantle. *Annual Reviews of Earth and Planetary Science*, **26**, 189–218.

Fisher JH, Barratt MW, Droste JB, Shaver RH (1988) Michigan Basin. In: *Sedimentary Cover-North American Craton* (ed. Sloss LL), pp. 361–82. *Geology of North America volume* D-2, Geological Society of America, Boulder, CO, USA.

Fontes JC, Garnier JM (1979) Determination of the initial ^{14}C activity of the total dissolved carbon: a review of the existing models and a new approach. *Water Resources Research*, **15**, 399–413.

Freeze RA, Cherry JA (1977) *Groundwater*. Prentice Hall, New Jersey.

Gieskes JM, Rogers WC (1973) Alkalinity determination in interstitial waters of marine sediments. *Journal of Sedimentary Research*, **43**, 272–7.

Ging PB, Long DT, Lee RW (1996) Selected geochemical characteristics of ground water from the Marshall Aquifer in the central Lower Peninsula of Michigan. United States Geological Survey, Water-Resources Investigations Report 94-4220.

Graham DW (2002) Noble gas isotope geochemistry of mid-ocean ridge and ocean island basalts: characterization of mantle

source reservoirs. *Reviews in Mineralogy and Geochemistry*, **47**, 247–317.
Grasby S, Osadetz K, Betcher R, Render F (2000) Reversal of the regional-scale flow system of the Williston basin in response to Pleistocene glaciation. *Geology*, **28**, 635–8.
Hall CM, Castro MC, Lohmann KC, Sun T (2012) Testing the noble gas paleothermometer with a yearlong study of groundwater noble gases in an instrumented monitoring well. *Water Resources Research*, **48**, W04517.
Han LF, Plummer LN (2013) Revision of Fontes & Garnier's model for the initial ^{14}C content of dissolved inorganic carbon used in groundwater dating. *Chemical Geology*, **351**, 105–14.
Heaton THE, Vogel JC (1981) "Excess air" in groundwater. *Journal of Hydrology*, **50**, 201–16.
Hilton DR, Porcelli D (2003) Noble gases as mantle tracers, in the Mantle and Core. In: *Treatise on Geochemistry* (eds Holland HD, Turekian KK), pp. 277–318. Elsevier, New York.
Hoaglund JR, Huffmann GC, Grannemann NG (2002) Simulation of Ground-Water Flow in the Glaciofluvial, Saginaw, Parma-Bayport, and Marshall Aquifers, Central Lower Peninsula of Michigan. United State Geological Survey Open-File Report: 2000-504.
Hoaglund JR, Kolak JJ, Long DT, Larson GJ (2004) Analysis of modern and Pleistocene hydrologic exchange between Saginaw Bay (Lake Huron) and the Saginaw Lowlands area. *Geological Society of America Bulletin*, **116**, 3–15.
Holland G, Gilfillan S (2013) Application of Noble Gases to the Viability of CO_2 Storage. In: *The Noble Gases as Geochemical Tracers* (ed Burnard P), pp. 177–223. Springer, Berlin, Heidelberg.
Kaufman S, Libby W (1954) The natural distribution of tritium. *Physical Review*, **93**, 1337–44.
Kazemi GA, Lehr JH, Perrochet P (2006) *Groundwater Age*. John Wiley & Sons Inc, Hoboken, NJ, USA.
Kipfer R, Aeschbach-Hertig W, Peeters F, Stute M (2002) Noble gases in lakes and ground waters. *Reviews in Mineralogy and Geochemistry*, **47**, 615–700.
Klump S, Grundl T, Purtschert R, Kipfer R (2008) Groundwater and climate dynamics derived from noble gas, ^{14}C, and stable isotope data. *Geology*, **36**, 395–8.
Kolak JJ, Long DT, Matty JM, Larson GJ, Sibley DF, Councell TB (1999) Ground-water, large-lake interactions in Saginaw Bay, Lake Huron: a geochemical and isotopic approach. *Geological Society of America Bulletin*, **111**, 177–88.
Long DT, Wilson TP, Takacs MJ, Rezabek DH (1988) Stable-isotope geochemistry of saline near-surface ground water: east-central Michigan basin. *Geological Society of America Bulletin*, **100**, 1568–77.
Ludin A, Weppernig R, Boenish G, Schlosser P (1998). Mass Spectrometric Measurement of Helium Isotopes and Tritium in Water Samples. L-DEO Technical Report.
Ma L, Castro MC, Hall CM (2004) A late Pleistocene-Holocene noble gas paleotemperature record in southern Michigan. *Geophysical research letters*, **31**, L23204.
Ma L, Castro MC, Hall CM, Walter LM (2005) Cross-formational flow and salinity sources inferred from a combined study of helium concentrations, isotopic ratios, and major elements in the Marshall aquifer, southern Michigan. *Geochemistry Geophysics Geosystems*, **6**, Q10004.
Ma L, Castro MC, Hall CM (2009) Crustal noble gases in deep brines as natural tracers of vertical transport processes in the Michigan Basin. *Geochemistry Geophysics Geosystems*, **10**, Q06001.
Mandle RJ (1986) Plan of Study for the Regional Aquifer Systems Analysis of the Michigan Basin. United States Geological Survey Open-File Report 86-494.
Mandle RJ, Westjohn DB (1989) Geohydrologic framework and ground-water flow in the Michigan basin. In: *Regional Aquifer Systems of the United States - Aquifers of the Midwestern Areas* (eds Swain LA, Johnson AI), pp. 83–110. American Resources Water Association Monograph Series, 13.
Martini AM (1997) *Hydrogeochemistry of Saline Fluids and Associated Water and Gas*. University of Michigan, Ann Arbor.
McIntosh JC, Walter LM, Martini AM (2004) Extensive microbial modification of formation water geochemistry: case study from a Midcontinent sedimentary basin, United States. *Geological Society of America Bulletin*, **116**, 743–59.
McIntosh JC, Garven G, Hanor JS (2011) Impacts of Pleistocene glaciation on large-scale groundwater flow and salinity in the Michigan Basin. *Geofluids*, **11**, 18–33.
McIntosh JC, Schlegel ME, Person M (2012) Glacial impacts on hydrologic processes in sedimentary basins: evidence from natural tracer studies. *Geofluids*, **12**, 7–21.
Menuge JF, Brewer ST, Seeger CM (2002) Petrogenesis of metaluminous A-type rhyolites from the St. Francois Mountains, Missouri and the Mesoproterozoic evolution of the southern Laurentian margin. *Precambrian Research*, **113**, 269–91.
Mook WG (1980) Carbon-14 in Hydrogeological Studies. In: *Handbook of Environmental Isotope Geochemistry* (eds Fritz P, Fontes JC), **1**, pp. 49–74, Elsevier Science.
Mook WG, Bommerson JC, Staverman WH (1974) Carbon isotope fractionation between dissolved bicarbonate and gaseous carbon dioxide. *Earth and Planetary Science Letters*, **22**, 169–76.
Morrison P, Pine J (1955) Radiogenic origin of the helium isotopes in rock. *Annals of the New york Academy of Science*, **62**, 71–92.
Neuzil CE, Provost AM (2014) Ice sheet load cycling and fluid underpressures in the Eastern Michigan Basin, Ontario, Canada. *Journal of Geophysical Research*, **119**, 8748–69.
Olcott PG (1992) *Ground Water Atlas of the United States*. United States Geological Survey, Reston, VA, USA.
O'Nions RK, Oxburgh ER (1983) Heat and helium in the Earth. *Nature*, **306**, 429–31.
Ozima M, Podosek FA (2002) *Noble Gas Geochemistry*. Cambridge University Press, New York.
Parker RL (1967) *Composition of Earth's crust, data of geochemistry*. United States Geological Survey Professional Papers 440-D.
Patriarche D, Castro MC, Goblet P (2004) Large-scale hydraulic conductivities inferred from three-dimensional groundwater flow and ^{4}He transport modeling in the Carrizo aquifer, Texas. *Journal of Geophysical Research*, **109**, B11202.
Person M, McIntosh J, Bense V, Remenda VH (2007) Pleistocene hydrology of North America: the role of ice sheets in reorganizing groundwater flow systems. *Reviews of Geophysics*, **45**, RG3007.
Pinti DL, Marty B (1998) The origin of helium in deep sedimentary aquifers and the problem of dating very old groundwaters. *Geological Society of London. Special Publication*, **144**, 53–68.
Reimer PJ, Baillie MGL, Bard E, Bayliss A, Beck JW, Blackwell PG, Ramsey CB, Buck CE, Burr GS, Edwards RL, Friedrich M, Grootes PM, Guilderson TP, Hajdas I, Heaton TJ, Hogg AG, Hughen KA, Kaiser KF, Kromer B, McCormac FG, Manning SW, Reimer RW, Richards DA, Southon JR, Talamo S, Turney CSM, van der Plicht J, Weyhenmeyer CE (2009) Intcal09 and Marine09 radiocarbon age calibration curves, 0–50,000 years cal BP. *Radiocarbon*, **51**, 1111–50.

Saar MO, Castro MC, Hall CM, Manga M, Rose TP (2005) Quantifying magmatic, crustal, and atmospheric helium contributions to volcanic aquifers using all stable noble gases: implications for magmatism and groundwater flow. *Geochemistry Geophysics Geosystems*, **6**, Q03008.

Schlosser P, Stute M, Dörr H, Sonntag C, Münnich KO (1988) Tritium/^{3}He dating of shallow groundwater. *Earth and Planetary Science Letters*, **89**, 353–62.

Speece M, Bowen T, Folcik J, Pollack H (1985) Analysis of temperatures in sedimentary basins: the Michigan Basin. *Geophysics*, **50**, 1318–34.

Starkey NA, Stuart FM, Ellam RM, Fitton JG, Basu S, Larsen LM (2009) Helium isotopes in early Iceland plume picrites: constraints on the composition of high ^{3}He/^{4}He mantle. *Earth and Planetary Science Letters*, **277**, 91–100.

Stueber AM, Walter LM (1991) Origin and chemical evolution of formation waters from Silurian-Devonian strata in the Illinois Basin, USA. *Geochimica et Cosmochimica Acta*, **55**, 309–25.

Stuiver M, Reimer PJ (1993) Extended ^{14}C database and revised CALIB 3.0 (super 14) C age calibration program. *Radiocarbon*, **35**, 215–30.

Stute M, Sonntag C, Deak J, Schlosser P (1992) Helium in deep circulating groundwater in the Great Hungarian Plain: flow dynamics and crustal and mantle helium fluxes. *Geochimica et Cosmochimica Acta*, **56**, 2051–67.

Thatcher LL (1962) The distribution of tritium fallout in precipitation over North America. *Hydrological Sciences Journal*, **7**, 48–58.

Tolstikhin I, Lehmann BE, Loosli HH, Gautschi A (1996) Helium and argon isotopes in rocks, minerals, and related ground waters: a case study in northern Switzerland. *Geochimica et Cosmochimica Acta*, **60**, 1497–514.

Torgersen T (1980) Controls on pore-fluid concentration of ^{4}He and ^{222}Rn and the calculation of ^{4}He/^{222}Rn ages. *Journal of Geochemical Exploration*, **13**, 57–75.

Torgersen T, Clarke WB (1985) Helium accumulation in groundwater, I: an evaluation of sources and the continental flux of crustal ^{4}He in the Great Artesian Basin, Australia. *Geochimica et Cosmochimica Acta*, **49**, 1211–8.

Torgersen T, Ivey GN (1985) Helium accumulation in groundwater. II: a model for the accumulation of the crustal ^{4}He degassing flux. *Geochimica et Cosmochimica Acta*, **49**, 2445–52.

Van Schmus WR (1992) Tectonic setting of the Midcontinent Rift system. *Tectonophysics*, **213**, 1–15.

Vugrinovich R (1986) Patterns of Regional Subsurface Fluid Movement in the Michigan Basin. Michigan Geological Survey Open File Report OFR 86-6.

Warrier RB, Castro MC, Hall CM (2012) Recharge and source-water insights from the Galapagos Islands using noble gases and stable isotopes. *Water Resources Research*, **48**, W03508.

Warrier RB, Castro MC, Hall CM, Lohmann KC (2013) Large atmospheric noble gas excesses in a shallow aquifer in the Michigan Basin as indicators of a past mantle thermal event. *Earth and Planetary Science Letters*, **375**, 372–82.

Weaver TR, Frape SK, Cherry JA (1995) Recent cross-formational fluid flow and mixing in the shallow Michigan Basin. *Geological Society of America Bulletin*, **107**, 697.

Weise SM (1986) *Heliumisotopen-Gehalte im Grumdwasser*. University of Munchen, Messung und Interpretation, Munchen, Germany.

Weise S, Moser H (1987) Groundwater dating with helium isotopes, *Isotope techniques in water resources development*. Proc. IAEA symposium, Vienna, (IAEA; Proceedings Series, STI/PUB/757), 105–26.

Weiss RF (1968) Piggyback sampler for dissolved gas studies on sealed water samples. *Deep Sea Research Part I: Oceanographic Research Papers*, **15**, 695–9.

Westjohn DB, Weaver TL (1996a) Hydrogeologic framework of Mississippian rocks in the central Lower Peninsula of Michigan. United States Geological Survey, Water-Resources Investigations Report 94-4246.

Westjohn DB, Weaver TL (1996b) Hydrogeologic framework of Pennsylvanian and Late Mississippian rocks in the central lower peninsula of Michigan. United States Geological Survey, Water-Resources Investigations Report 94-4107.

Westjohn DB, Weaver TL (1998) Hydrogeologic framework of the Michigan Basin regional aquifer system. United States Geological Survey Professional Paper 1408.

Westjohn DB, Weaver TL, Zacharias KF (1994) Hydrogeology of Pleistocene glacial deposits and Jurassic "red beds" in the central lower peninsula of Michigan. United States Geological Survey, Water-resources investigations report 93-4152.

William JH, Richard LK, Norbert WO (1975) Geophysical studies of basement geology of southern Peninsula of Michigan. *AAPG Bulletin*, **59**, 1562–84.

Wilson TP (1989) *Origin and Geochemical Evolution of the Michigan Basin Brine*. Michigan State University, East Lansing.

Wilson TP, Long DT (1993a) Geochemistry and isotope chemistry of CaNaCl brines in Silurian strata, Michigan Basin, U.S.A. *Applied Geochemistry*, **8**, 507–24.

Wilson TP, Long DT (1993b) Geochemistry and isotope chemistry of Michigan Basin brines: devonian formations. *Applied Geochemistry*, **8**, 81–100.

SUPPORTING INFORMATION

Additional Supporting Information may be found in the online version of this article:

Text S1. Sensitivity Tests of the ^{4}He Flux J_0 and Velocity v_x in the Saginaw Aquifer.

Figure S1. Model results for sensitivity tests of the ^{4}He flux value for the Saginaw aquifer: calculated $^4He_{exc}$ curves for five different orders of magnitude of the flux value, between 6.1×10^{-5} and 6.1×10^{-9} cm^3 STP cm^2 yr^{-1} and a constant velocity value of 5.37 m yr^{-1}.

Figure S2. Model results for a flux value of 6.1×10^{-7} cm^3 STP cm^2 yr^{-1} and velocity values of (A) 0.537 and (B) 53.7 m yr^{-1} in the Saginaw aquifer, respectively.